

LAPPEENRANTA UNIVERSITY OF TECHNOLOGY  
FACULTY OF TECHNOLOGY  
DEPARTMENT OF ELECTRICAL ENGINEERING

**MASTER'S THESIS**

**DESIGN AND COMPARISON OF MIXED  $H_\infty/H_2$   
CONTROLLER FOR AMB SYSTEM**

Examiners D.Sc. Tuomo Lindh, PhD. Victor Vtorov

Supervisors Rafal Jastrzebski, Alexander Smirnov

Author Armen Madoyan  
Punkkerikatu 5A 19  
53850 Lappeenranta  
armen.madoyan@lut.fi

Lappeenranta, May 2009

**Abstract**

Lappeenranta University of Technology

Faculty of Technology

Electrical Engineering

Armen Madoyan

**Design and Comparison of Mixed  $H_\infty/H_2$  Controller for AMB System**

Master's thesis

2009

65 pages, 34 pictures, 5 tables and 3 appendixes

Examiners: Dr.Sc Tuomo Lindh and PhD. Victor Vtorov

Keywords: active magnetic bearings, multi-objective control, function *hinfmix()*, mixed  $H_2/H_\infty$  ( $H_{sub2}/H_{inf}$ ) controller, robust control, robust performance and stability.

This master's thesis is focused on the active magnetic bearings control, specifically the robust control. As carrying out of such kind of control used mixed  $H_2/H_\infty$  controller. So the goal of this work is to design it using Robust Control Toolbox™ in MATLAB and compare its performance and robustness with  $H_\infty$  robust controller characteristics. But only one degree-of-freedom controller is considered.

**Acknowledgments**

I would like to express my sincere appreciation to people who assisted and those who did not directly take part in this work.

First of all, I want to thank my supervisors Dr.Sc Rafal Jastrzebski and Mr.Sc Alexander Smirnov for the possibility to work on such an interesting project, for the answers to my endless questions.

I want to thank Professor Tuomo Lindh for his condescension and understanding.

I am grateful to Professor Victor Vtorov for his participation and for his wise suggestions.

Person who made my study at Lappeenranta University of Technology possible is Julia Vauterin. Thank You very much.

Special thanks to my friends at Punkkerikatu 5A for their support in anxious times and for joyfulness You brought me.

I am immensely grateful to my parents and sister for their care and love, and special thanks to my niece.

Lappeenranta, May 2009

Armen Rubenovich Madoyan.

## Table of contents

1	INTRODUCTION	7
2	THEORETICAL BACKGROUND OF ROBUST CONTROL	10
2.1	Reasons for robust control	10
2.2	Robust control approaches	12
2.3	Measures of robustness	14
2.3.1	Robust Stability	14
2.3.2	Robust performance	16
2.4	Mixed H <sub>2</sub> /H <sub>∞</sub>	18
3	AMB APPLICATION	23
3.1	Introducing the AMB system	23
3.2	Dynamic model of AMB rotor system	25
4	DESIGN OF MIXED H <sub>∞</sub> /H <sub>2</sub> CONTROLLER	27
4.1	Control specifications	27
4.1.1	Design schemes	27
4.1.2	Weighting functions	31
4.2	Design procedure	35
4.3	Results	41
4.3.1	Simulation	43
4.3.2	Robust stability check	45
4.3.3	Robust performance check	47
4.4	Comparison of mixed H <sub>2</sub> /H <sub>∞</sub> and H <sub>∞</sub> controllers	50
5	Conclusions	53
	References	55

## Nomenclature

$d_i$	input disturbance
$d_o$	output disturbance
$e$	error
$F$	closed-loop transfer function/closed-loop transfer function matrix
$G$	plant transfer function/plant transfer function matrix
$G_p$	perturbed plant transfer function/perturbed plant transfer function matrix
$I$	unity matrix
$K$	transfer function of controller/transfer function of controller matrix
$L$	loop transfer function/ loop transfer function matrix
$L_p$	perturbed loop transfer function/ perturbed loop transfer function matrix
$n$	measurement noise
$P$	transfer function of generalized plant/transfer function of generalized plant matrix
$r$	reference signal (scalar, vector)
$S$	sensitivity transfer function/ sensitivity transfer function matrix
$T$	complementary sensitivity transfer function
$u$	control signal
$v$	measured signals (scalar, vector)
$w$	input signals (scalar, vector)
$w_I, W_I$	input uncertainty weighting function/ input uncertainty weighting function matrix
$w_p, W_p$	output weighting function/ output weighting function matrix
$w_u, W_u$	control signal weighting function/ control signal weighting function matrix
$w_x, W_x$	state variables weighting function/ state variables weighting function matrix
$x$	space coordinates, vector of displacements or state variables in state-

	space representation
$y$	vector of outputs in state-space representation or vector of measurements
$y_m$	measured vector of outputs in state-space representation or vector of measurements
$z_\infty$	vector of outputs optimized by $h_\infty$ - norm
$z_2$	vector of outputs optimized by $h_2$ - norm

## 1 Introduction

From ancient times, people have sought to achieve perfection in everything. In all its endeavors. Ever since the wheel had been invented, one of the greatest inventions of mankind, and other rotating machines, people started to invent a different ways to reduce the shaft friction to reduce energy loss. The lowest friction - it is it's absence. Thus, for these purposes, levitation was used. *Levitation* (from Latin levitas "lightness") is the process by which an object is suspended against gravity, in a stable position, without physical contact. For levitation on Earth, first, a force is required directed vertically upwards and equal to the gravitational force; second, for any small displacement of the levitating object, a returning force should appear to stabilize it. The magnetic forces were used to keep the levitation stable as much as possible. So, levitation used to maintain the shaft in the air. This method is implemented in the rotating machinery in the form of magnetic bearings. For the rotor position control two types of magnetic bearings, radial and axial, are applied.

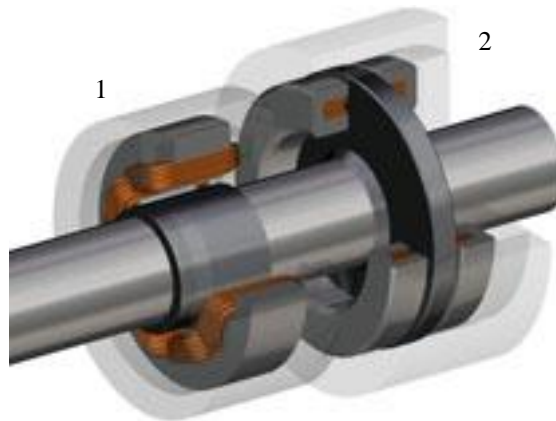


**Fig. 1:** Radial (1) and axial (2) active magnetic bearings (<http://www.s2m.fr/E/2-technology/magnetic-bearings-technology.html>.)

Along with the development of magnetic bearings, problem of controlling the shaft position became relevant.

The control theory is full of different automatic control methods. The most widely used methods were based on a comparison of the obtained results with the initial data, reference values, and the so-called system with feedback. Below are the modern methods of control:

- **Adaptive control** uses on-line identification of the process parameters, or modification of controller gains, hence providing robustness of the system (Besekersky 2004).
- A **Hierarchical control** system is a type of control system in which a set of devices and governing software is arranged in a hierarchical tree. When the links in the tree are implemented by a computer network, then that hierarchical control system is also a form of Networked control system (Besekersky 2004).
- **Intelligent control** use various AI computing approaches like neural networks, Bayesian probability, fuzzy logic, machine learning, evolutionary computation and genetic algorithms to control a dynamic system (Miroshnik 2000).
- **Optimal control** is a particular control technique in which the control signal optimizes a certain "cost index": for example, in the case of a satellite, the jet thrusts needed to bring it to desired trajectory that consume the least amount of fuel (Besekersky 2004).
- **Robust control** deals explicitly with uncertainty in its approach to controller design. Controllers designed using robust control methods tend to be able to cope with small differences between the true system and the nominal model used for design. Robust methods aim to achieve robust performance and/or stability in the presence of small modeling errors (Besekersky 2004, Miroshnik 2000).



- **Stochastic control** deals with control design with uncertainty in the model. In typical stochastic control problems, it is assumed that there exist random noise and disturbances in the model and the controller, and the control design must take into account these random deviations (Besekersky 2004).

In this thesis a method a robust control will be considered for axial AMB system. Robust control - a set of methods of control theory, the aim of which is a synthesis of the controller, which ensures good control quality (e.g., stability), when the plant is different from predicted model or its mathematical model is unknown. Systems possessing the property of robustness are called robust systems. In this work, for the implementation of robust control mixed  $H_\infty/H_2$  controller was chosen to be designed and compared with  $H_\infty$  controller that was designed as well.

## 2 Theoretical background of robust control

The main objective of the synthesis of robust control systems is to find control law, which preserves the system's output variables and the error signals in the specified permissible limits despite the presence of an uncertainty in the controlled system. Uncertainties may take any form, but the most significant are noise, nonlinearity and inaccuracy in the knowledge of the transfer function of the plant.

Consequently a definition of robust control could be stated as:

*“Design a controller such that some level of performance of the controlled system is guaranteed irrespective of changes in the plant dynamics within a predefined class.”* (Damen 2002).

### 2.1 Reasons for robust control

Modern control techniques allow engineers to optimize control systems for cost and performance. However, the optimal control does not always correctly responds to changes in the system or the environment. Robust control theory provides set of methods for measuring performance changes in control system with changing the parameters of the system. Application of those methods is important in developing of reliable embedded systems. The purpose is to obtain the system which is:

- insensitive to variations of parameters (uncertainties);
- able to maintain its stability and performance (Rollins 1999)

"Robust control refers to the control of unknown plants with unknown dynamics subject to unknown disturbances" (Rollins 1999). Obviously, the key question of robust control systems is uncertainty and how the control system can deal with

this issue. Figure 2.1 shows the simple control loop. Uncertainty is shown entering the system in three places:

- at the input of the plant as the disturbance ( $d_i$ );
- at the output of the plant as the disturbance ( $d_o$ );
- and the measuring noise ( $n$ ).

In practice there is difference between the true perturbed plant  $G'$  and the plant model  $G$ . It is caused by a number of different sources (perturbations). This work, in case of active magnetic bearings, is focused on uncertainties in parameters of the system, input and output disturbances.

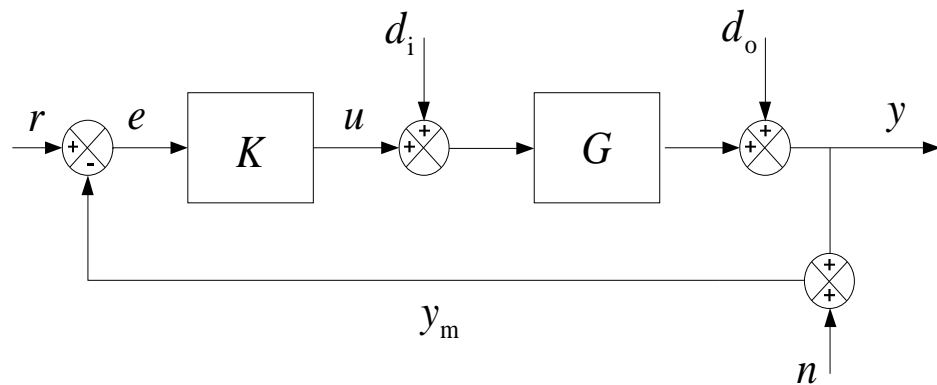


**Fig. 2.1:** Closed-loop control system with uncertainty.

In the robust control problem formulation, the objective is to keep the transfer functions between disturbances and chosen outputs small. In this work it will be guaranteed by  $H_\infty$  and  $H_2$  norms. To this end have been introduced special sensitivity functions:

- Input-to-plant loop transfer function  $L_I = KG$  ;
- Input sensitivity  $S_I = (1 + L_I)^{-1}$  ;
- Input complementary sensitivity  $T_I = L_I (1 + L_I)^{-1}$  ;
- Output-to-plant loop transfer function  $L_o = GK$  ,

- Output sensitivity  $S_o = (1 + L_o)^{-1}$ ;
- Output complementary sensitivity  $T_o = L_o (1 + L_o)^{-1}$ .

It is important to understand that the designer of control system have a little control over the uncertainty in the plant. The designer creates a system of control that is based on a model plant. However, the control completes over the real system, not on the model of that system (Rollins 1999).

## 2.2 Robust control approaches

The goal of robust design is a synthesis of the controller, which would satisfy the criterion of robustness. Since 50-ies of the XX century, a set of procedures and algorithms were developed to solve the problem of robust synthesis. Robust control system can combine features of both classical control, and adaptive and fuzzy.

Table 1. Controller synthesis methods.

Technology name	Preference	Drawback
$H_\infty$ - synthesis	<ul style="list-style-type: none"> <li>• Works both with stability and with sensitivity of the system;</li> <li>• Closed loop is always stable;</li> <li>• One-pass algorithm for direct synthesis;</li> </ul>	<ul style="list-style-type: none"> <li>• Requires special attention to the parametric robustness of the plant;</li> </ul>
$H_2$ - synthesis	<ul style="list-style-type: none"> <li>• Works both with stability and with sensitivity of the system;</li> <li>• Closed loop is always stable;</li> <li>• The exact formation of the transfer function of controller;</li> </ul>	<ul style="list-style-type: none"> <li>• A large number of iterations;</li> </ul>
<ul style="list-style-type: none"> <li>• LQG – synthesis</li> </ul>	<ul style="list-style-type: none"> <li>• Uses available information about the noise;</li> </ul>	<ul style="list-style-type: none"> <li>• Not guaranteed stability;</li> <li>• Requires an exact model of the object;</li> <li>• Large number of iterations;</li> </ul>
<ul style="list-style-type: none"> <li>• LQR – synthesis</li> </ul>	<ul style="list-style-type: none"> <li>• Guaranteed robust stability,</li> <li>• Inertialless regulator.</li> </ul>	<ul style="list-style-type: none"> <li>• Need feedback on the entire state vector;</li> <li>• Requires an exact model of the object;</li> <li>• Large number of iterations;</li> </ul>
$\mu$ – synthesis	<ul style="list-style-type: none"> <li>• Works with a wide class of uncertainties.</li> </ul>	<ul style="list-style-type: none"> <li>• High order controller.</li> </ul>

Table 1 lists the basic technologies of synthesis of robust control systems. Actually  $H_2$  (LQG, LQR) controllers are not robust control methods, and as in this work is designed mixed  $H_\infty/H_2$  controller their properties are considered below.

**H-infinity** (" $H_\infty$ ") methods are used in control theory to synthesize controllers achieving robust performance or stabilization. To use  $H_\infty$  methods, a control designer expresses the control problem as a mathematical optimization problem and then finds the controller that meets the requirements.  $H_\infty$  techniques have the advantage over classical control techniques in that they are readily applicable to problems involving multivariable systems with cross-coupling between channels; disadvantages of  $H_\infty$  techniques include the level of mathematical understanding needed to apply them successfully and the need for a reasonably good model of the system to be controlled.

It is well accepted that  **$H_2$  norm** is a good measure for system performance.  $H_2$  performance is useful to deal with stochastic aspects especially, such as measurement noise and random disturbance. However, the  $H_2$  control design is based on the assumption that the system is exactly modeled, which is impractical (Zhao 2006).

**LQG (linear quadratic Gaussian)** controller is simply a combination of Kalman filter with a linear-quadratic regulator (LQR). The principle of the separation assures that they can be designed and calculated independently. LQG control applies to both linear time-invariant systems as well as linear time-varying systems. Application of linear time-invariant systems is well known. Application to linear time-varying systems enables design of linear feedback controllers for non-linear uncertain systems (Athuts 1971).

**LQR (Linear quadratic regulator)** in theory one of the best types of controls, using quadratic functional quality. The problem, in which the dynamical system described by linear differential equations, while the quality is a quadratic

functional, called the problem of linear-quadratic control. One of the main results in the theory is that the solution is provided by the linear-quadratic regulator (LQR), a feedback controller. The LQR is an important part of the solution to the LQG problem. Like the LQR problem itself the LQG problem is one of the most fundamental problems in control theory (Kwakernaak 1972).

### 2.3 Measures of robustness

Within the context of controller design, *nominal* properties concern the characteristics of the system when the model of the controlled process is assumed to duplicate real process behavior. On the other hand, *robustness* properties refer to those of a system in the presence of process-model perturbations.

In the first place in the designing of the control system is to provide the system stability and desired level of performance. Thus, the conditions of nominal stability and nominal performance should be satisfied. However, before applying the controller to real system, it is necessary to design it on a model of the system under conditions of robust stability and robust performance (Thang 2002).

#### 2.3.1 Robust Stability

Here considered the uncertain feedback system in Figure 2.3 with multiplicative uncertainty of magnitude  $|w_I(j\omega)|$ .

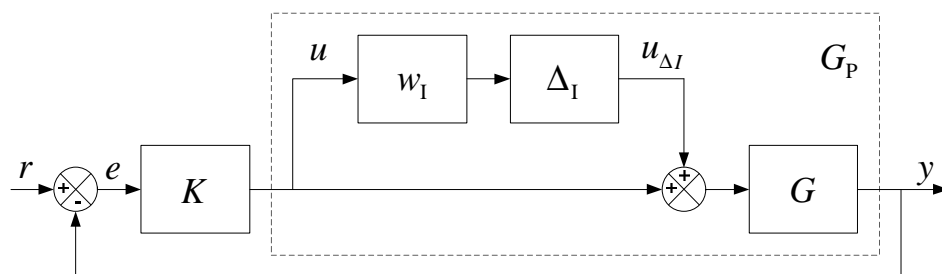


**Fig. 2.3:** Feedback system with multiplicative uncertainty.

And it has new loop transfer function with uncertainty:

$$L_P = G_P K = GK(1 + w_I \Delta_I) = L + w_I L \Delta_I, \quad |\Delta_I(j\omega)| \leq 1, \forall \omega \quad (2.3)$$

To simplify the process of deriving the robust stability condition was assumed that nominal closed-loop system is stable and also the loop transfer function  $L_p$  is stable too. According to the Nyquist stability condition the  $L_p$  should not encircle the point -1,  $\forall L_p$ .

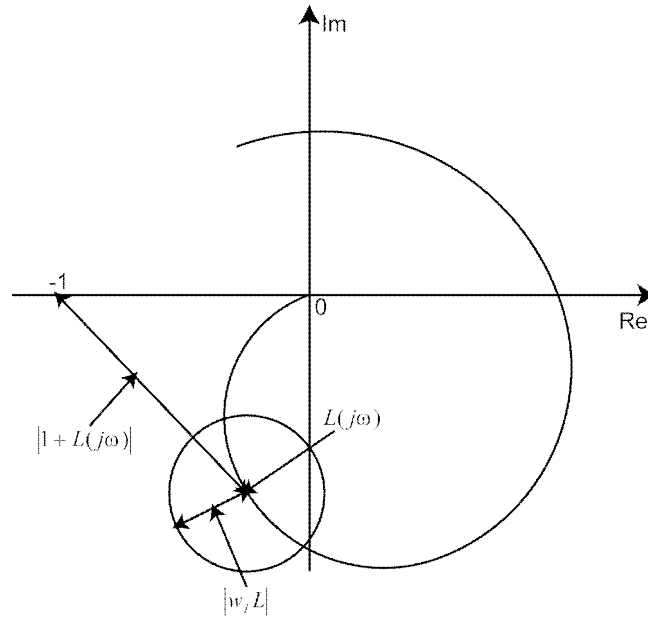


**Fig. 2.4:** Nyquist plot of  $L_p$  for robust stability.

As can be seen in the figure 2.4 the distance from the point -1 to the centre of the circles with radius  $|w_I L|$  is  $|1 + L|$ . For robust stability none of the circles should cover -1, consequently:

$$RS \Leftrightarrow |w_I L| < |1 + L|, \forall \omega \quad (2.4)$$

$$\Leftrightarrow \left| \frac{w_I L}{1 + L} \right| < 1, \forall \omega \Leftrightarrow |w_I T| < 1, \forall \omega \quad (2.5)$$

$$\stackrel{def}{\Leftrightarrow} \|w_I T\|_{\infty} < 1 \quad (2.6)$$

Thus, obtained the robust stability requirement for the system with multiplicative uncertainty:

$$RS \Leftrightarrow |T| < 1/|w_I|, \forall \omega \quad (2.7)$$

The graphical derivation of robust stability was considered above (Skogestad 2005). Also condition for robust stability could be defined as follow:

*The system is stable for all uncertainties which satisfy the norm bound  $\|\Delta\|_\infty \leq 1$  if and only if the nominal closed-loop transfer function  $F$  is stable and*

$$\|F\|_\infty \leq 1 \quad (2.8)$$

So, keeping in mind conditions of this theorem, the robust stability of the system under consideration is guaranteed (Toivonen).

### 2.3.2 Robust performance.

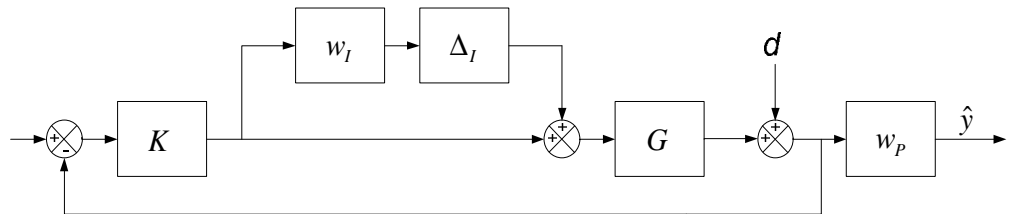


**Fig. 2.5:** Diagram for robust performance with multiplicative uncertainty.

To achieve the robust performance the conditions of nominal performance

$$NP \Leftrightarrow |w_p S| < 1, \forall \omega \Leftrightarrow |w_p| < |1 + L|, \forall \omega \quad (2.9)$$

must be satisfied, but for all possible plants, thus we get the conditions:



$$RP \stackrel{def}{\Leftrightarrow} |w_p S_p| < 1, \forall \omega, \forall S_p \quad (2.10)$$

$$\Leftrightarrow |w_p| < |1 + L_p|, \forall \omega, \forall L_p \quad (2.11)$$

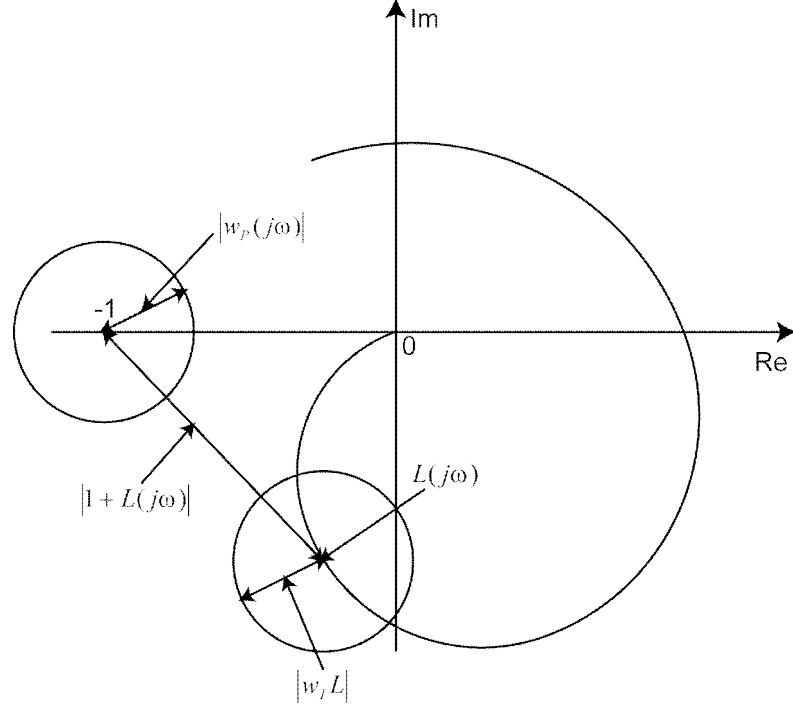


**Fig. 2.6:** Nyquist plot illustration of robust performance condition  $|w_p| < |1 + L_p|$ .

For guarantee robust performance required that all possible  $L_p(j\omega)$  should not cross the circle with radius  $|w_p(j\omega)|$  centred on  $-1$ . The distance between centres of two discs which are located on  $-1$  and  $L(j\omega)$  is  $|1 + L|$ , thus, the robust performance condition becomes:

$$RP \Leftrightarrow |w_p| + |w_I L| < |1 + L|, \forall \omega \quad (2.12)$$

$$\Leftrightarrow |w_p (1 + L)^{-1}| + |w_I L (1 + L)^{-1}| < 1, \forall \omega \quad (2.13)$$

or

$$\boxed{RP \Leftrightarrow \max_{\omega} (|w_p S| + |w_I T|) < 1} \quad (2.14)$$

Summarizing all the above-said about nominal performance, robust stability and robust performance we get:

$$NP \Leftrightarrow |w_p S| < 1, \forall \omega \quad (2.15)$$

$$RS \Leftrightarrow |w_I T| < 1, \forall \omega \quad (2.16)$$

$$RP \Leftrightarrow |w_p S| + |w_I T| < 1, \forall \omega \quad (2.17)$$

From this can be seen that for *robust performance* must be satisfied *robust stability* and *nominal performance conditions* and that if there is *robust performance* it follows *nominal performance* and *robust stability*.

#### 2.4 Mixed $H_2/H_\infty$

The mixed performance and robustness of the control problems has been the object of much attention today. These various objective problems rarely encompass single synthesis criterion. While some tracking and robustness are best captured by the  $H_\infty$  criterion, noise insensitivity and energy optimization is more naturally expressed in  $H_2$  terms. In this work the mixed  $H_2/H_\infty$  is designed for SISO linear time invariant system of axial AMB system as shown in the figure 2.7. It is multi-objective state feedback synthesis, which considers:

- §  $H_\infty$  performance (convenient to enforce robustness to model uncertainty and to express frequency-domain specifications such as bandwidth, low-frequency gain and roll-off);
- §  $H_2$  performance (useful to handle stochastic aspects such as measurement noise and random disturbance);
- § Pole placement constraint (desirable to enforce some minimum decay rate or closed-loop damping via regional pole assignment).

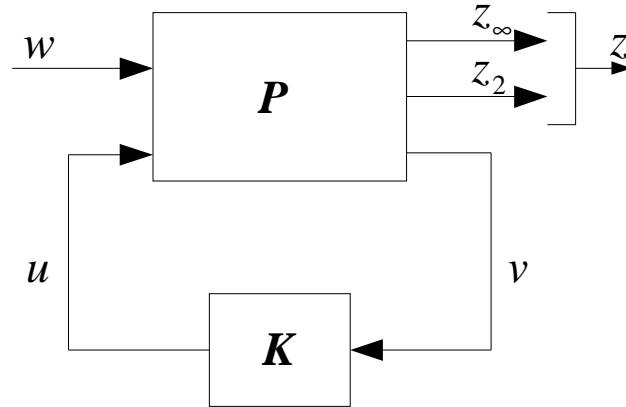


**Fig. 2.7:** General control configuration.

Where  $u$  - the control variables,  $v$  - the measured variables,  $w$  - the external signals (disturbances, commands...),  $z$  - output signal.  $P$  is generalized plant:

$$P = \begin{bmatrix} A & B_1 & B_2 \\ C_1 & D_{11} & D_{12} \\ C_2 & D_{21} & D_{22} \end{bmatrix} \quad (2.20)$$

Generalized plant  $P$  includes the plant model  $G$ , the interconnection structure, and the designer specified weighting functions. Where  $D_{11} = 0$ ,  $D_{22} = 0$ ,

$D_{12} = \begin{bmatrix} 0 \\ I \end{bmatrix}$  and  $D_{21} = [0 \quad I]$ . These are the typical assumptions made in  $H_2$  and

$H_\infty$  problems. State-space realization of the plant:

$$\begin{aligned} \dot{\mathbf{x}} &= A\mathbf{x} + B_1\mathbf{w} + B_2u \\ z_\infty &= C_1\mathbf{x} + D_{11}\mathbf{w} + D_{12}u \\ z_2 &= C_2\mathbf{x} + D_{21}\mathbf{w} + D_{22}u \\ \mathbf{y} &= C_y\mathbf{x} + D_yu \end{aligned} \quad (2.18)$$

Taken separately, our three design objectives have the following formulation:

**$H_\infty$  performance:** let  $T$  is the transfer function from  $\mathbf{w}$  to  $z_\infty$ . And the closed-loop RMS value of  $T$  does not exceed  $\gamma$  if and only if there exists a symmetric matrix  $X_\infty$  such that:

$$\begin{pmatrix} (A + B_2 K)X_\infty + X_\infty(A + B_2 K)^T & B_1 & X_\infty(C_1 + D_{12}K)^T \\ B_1^T & -I & D_{11}^T \\ (C_1 + D_{12}K)X_\infty & D_{11} & -\gamma^2 I \end{pmatrix} < 0$$

$$X_\infty > 0$$

**$H_2$  performance:** the closed-loop  $H_2$  norm of  $T_2$  does not exceed  $\gamma$  if and only if there exists two symmetric matrices  $X_2$  and  $Q$  such that:

$$\begin{pmatrix} (A + B_2 K)X_2 + X_2(A + B_2 K)^T & B_1 \\ B_1^T & -I \end{pmatrix} < 0$$

$$\begin{pmatrix} Q & (C_2 + B_{22}K)X_2 \\ X_2(C_2 + B_{22}K)^T & X_2 \end{pmatrix} < 0$$

$$\text{Trace}(Q) < v^2$$

**Pole placement performance:** the main reason of seeking pole clustering in specific region of the left half plane is to control the transient behavior of a linear system, as it is related to the location of poles. The closed-loop poles lie in the region  $D = \{z \in \mathbb{C} : L + Mz + M^T \bar{z}\}$ , where  $L = L^T = \{\lambda_{ij}\}_{1 \leq i, j \leq m}$ ,  $M = M^T = \{\mu_{ij}\}_{1 \leq i, j \leq m}$ , if and only if there exists a symmetric matrix  $X_{pol}$  satisfying:

$$\left[ \lambda_{ij} X_{pol} + \mu_{ij} (A + B_2 K) X_{pol} + \mu_{ij} X_{pol} + \mu_{ij} X_{pol} (A + B_2 K)^T \right]_{1 \leq i, j \leq m} < 0$$

$$X_{pol} > 0$$

System illustrated in the figure.2.7 also described by set of equations:

$$\begin{bmatrix} \mathbf{z} \\ \mathbf{v} \end{bmatrix} = \mathbf{P}(s) \begin{bmatrix} \mathbf{w} \\ \mathbf{u} \end{bmatrix} = \begin{bmatrix} \mathbf{P}_{11}(s) & \mathbf{P}_{12}(s) \\ \mathbf{P}_{21}(s) & \mathbf{P}_{22}(s) \end{bmatrix} \begin{bmatrix} \mathbf{w} \\ \mathbf{u} \end{bmatrix}, \quad (2.18)$$

$$\mathbf{u} = \mathbf{K}(s)\mathbf{v}. \quad (2.19)$$

The transfer function from  $\mathbf{w}$  to  $\mathbf{z}$ :

$$\mathbf{z} = F_l(\mathbf{P}, \mathbf{K})\mathbf{w}, \quad (2.21)$$

where

$$F_l(\mathbf{P}, \mathbf{K}) = \mathbf{P}_{11} + \mathbf{P}_{12}\mathbf{K}(\mathbf{I} - \mathbf{P}_{22}\mathbf{K})^{-1}\mathbf{P}_{21}. \quad (2.22)$$

Exactly, the minimization of the  $H_2$  and  $H_\infty$  norms of  $F_l(\mathbf{P}, \mathbf{K})$  is the objective of  $H_2$  and  $H_\infty$  control respectively.

In general the  $H_2$  optimization problem is to find a stabilizing controller  $\mathbf{K}$  which minimizes

$$\|F(s)\|_2 = \sqrt{\frac{1}{2\pi} \int_{-\infty}^{\infty} F(j\omega)F(j\omega)^T d\omega}, \quad F = F(\mathbf{P}, \mathbf{K}) \quad (2.23)$$

In general the  $H_\infty$  optimization problem is to find all stabilizing controllers  $\mathbf{K}$  which minimize

$$\|F_l(\mathbf{P}, \mathbf{K})\|_\infty = \max_{\omega} \bar{\sigma}(F_l(\mathbf{P}, \mathbf{K})(j\omega)). \quad (2.24)$$

In the subsequent development of  $H_\infty$  technology, it became clear that the two approaches of optimization  $H_2$  and  $H_\infty$  relate more than it seemed. The robust  $H_2$

performance problem is more complex, as it mixes two different system norms; the  $H_2$ -norm associated with performance, and the  $H_\infty$  norm associated with robustness. This leads to a mixed  $H_2/H_\infty$  problem, for which special solution methods have been developed.

### **3 AMB application**

#### **3.1 Introducing the AMB system**

The idea of contactless support has been interesting mankind for centuries. The first thing that comes to mind is to use a magnetic field. However, it is not so simple. There are a lot of laws complicate the application of magnetic field for these purposes in nature. The most famous is the Earnshaw theorem, which states that an object in the passive magnetic field may be in some stable position only when the material of object is diamagnetic or superconducting. This fact limits the engineering application of passive fields, as well as the majority of machines made from ferromagnetic. Nevertheless, the passive field of permanent magnets can be used to maintain the object with multiple degrees of freedom, but only if at least one degree of freedom is controlled by other means.

An active magnetic bearing system is a collection of electromagnets used to suspend an object and stabilization of the system is performed by feedback control. The system consists of a floating mechanical rotor and electromagnets that provide the controlled dynamic force and thus allowing the suspended object to move in its predefined functionality. Due to this contactless operation, AMB system has many advantages for high-speed, high-temperature and clean-environment applications. Moreover, adjustable stiffness and damping characteristics also make the AMB suitable for elimination of vibration in the system. Although the system is complex, the advantages it offers in some cases outweigh the design complexity.

The AMB rotor system has 6 degrees of freedom. Figure 3.1 illustrates the principle of active magnetic bearings in one coordinate system. Electromagnets from opposite sides pull the rotor and the total force is the sum of these electromagnets forces. The interaction of the ferromagnetic rotor and electromagnets is unstable. Therefore, it is necessary to control the position of the rotor by controlling the currents in electromagnets winding. Rotor position

can be defined with position sensor or evaluated from the winding currents. In the studied application 5 degrees of freedom of the rotor are controlled by four radial and one axial bearing. And the sixth degree of freedom controlled by the motor.

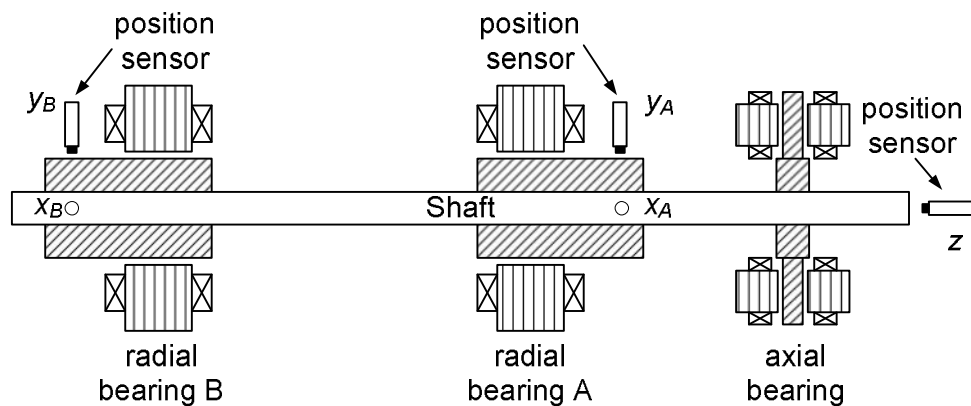


**Fig. 3.1:** Cross section of an active magnetic bearing.

To prevent the eddy currents in the radial bearings the rotor consists of a solid core and the external part is made of laminated steel. The winding of an electromagnet is made of regular copper wire. The axial bearings are separate magnets manufactured from solid iron.

Application areas of magnetic bearings are still steadily expanding because of these practically useful features. A few of the AMB applications that receive huge attentions from many research groups around the world are the flywheel energy and storage device, turbo molecular pump, compressor, Left Ventricle Assist Device (LVAD) and artificial heart. For the LVAD and artificial hearts applications particularly, the present of any debris or dust resulted from any mechanical contact is strictly unacceptable since these particles can block up the circulating blood that definitely will cause more injurious effects to human.



### 3.2 Dynamic model of AMB rotor system

The suitable AMB rotor system model is necessary to find the exact controller.

A system model of axial AMBs consists of the following elements:

- state space model of the rotor;
- actuator (electromagnets and amplifiers) model;

It is an uncertain system model with one input, one output (SISO) and three states. At the input of this system the control current is fed. As the output of the system it has the position of the rotor, determined by sensors. It is provided, taking into account the parameters uncertainties, in state-space representation:

$$\begin{cases} \dot{\mathbf{x}} = \mathbf{A}\mathbf{x} + \mathbf{B}u, \\ \mathbf{y} = \mathbf{C}\mathbf{x} + \mathbf{D}u, \end{cases} \quad (3.1)$$

where

$$\mathbf{A} = \begin{bmatrix} -566.6 & 0 & 0 \\ 0 & 0 & 262,9 \\ 262,9 & 87,65 & 0 \end{bmatrix}, \mathbf{B} = \begin{bmatrix} 566.6 \\ 0 \\ 0 \end{bmatrix}, \quad (3.2)$$

$$\mathbf{C} = [0 \quad 1 \quad 0], \mathbf{D} = [0] \quad (3.3)$$

In particular considered model has following uncertainties:

- $\omega_{bw}$  - uncertainty in actuator bandwidth, which is based on the actuator saturation;
- $k_i, k_x$  - uncertainty in current and position stiffnesses;
- $m$  - uncertainty in mass;
- *sennon* - 5% nonlinearity in position sensors.

Table 2 represents the properties of considered uncertainties in the model of the system.

Table 2. Properties of uncertainties.

Parameter Property	$\omega_{bw}$	$k_i$	$k_x$	$m$	$sennon$
Nominal value	567	213	$1.07 \cdot 10^6$	46.2	1
Range or Variability	[536.742 596.379]	[-10 10]%	[-20 20]%	[-2 2]%	[-5 5]%

The uncertain axial AMB system model is provided by Jastrzebski (2007).

## 4 Design of mixed $H_\infty/H_2$ controller

In robust control theory,  $H_2$  performance and  $H_\infty$  performance are two important specifications.  $H_\infty$  performance is convenient to enforce robustness to model uncertainty;  $H_2$  performance is useful to handle stochastic aspects such as measurement noise and capture the control cost. In time-domain aspects, satisfactory time response and closed-loop damping can often be achieved by enforcing the closed-loop poles into specialized pole placement region. Combining them together to form so-called mixed  $H_2/H_\infty$  design with pole placement allows for more flexible and accurate specification of closed-loop behavior (Chen 2006). Linear matrix inequalities technique is often considered for this kind of multi-objective synthesis.

### 4.1 Control specifications

The analysis of sensitivity functions gives quantitative information about how sensitive the nominal model is to uncertainties of the plant parameters or external disturbances.

#### 4.1.1 Design schemes

Mixed-sensitivity is the name given to transfer function shaping problems in which the sensitivity function  $S_o = (1 + GK)^{-1}$  is shaped along with one or more other closed-loop transfer functions such as  $KS$  or the complementary sensitivity function  $T_o$ .

Sensitivity functions which should be shaped depend on our objectives. The main objective in AMB system control is to reject a disturbance  $d$  entering at the rotor shaft. Hence, to this problem it makes sense to shape the closed-loop transfer functions  $S$  and  $KS$ . There are two types of these schemes: with reference signal as the input to the plant (Figure 4.7) and with disturbance signal as the input of the plant (Figure 4.6).

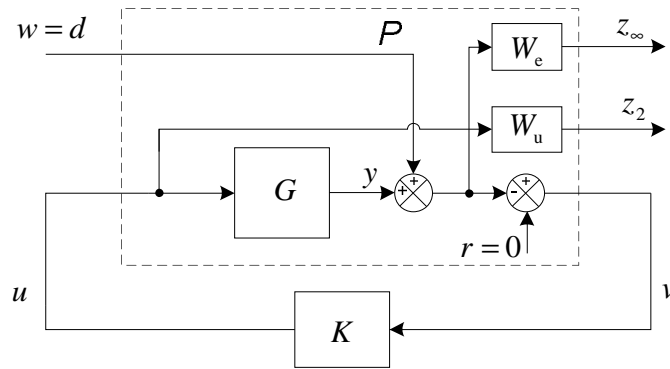


**Fig. 4.6:**  $S/KS$  mixed sensitivity optimization in standard form (regulation).

$S/KS$  scheme where external input is a reference command  $r$  used in tracking problem. The error signals are  $z_\infty = z_e = W_e e = W_e S w$  and  $z_2 = z_u = W_u u = W_u K S w$ .

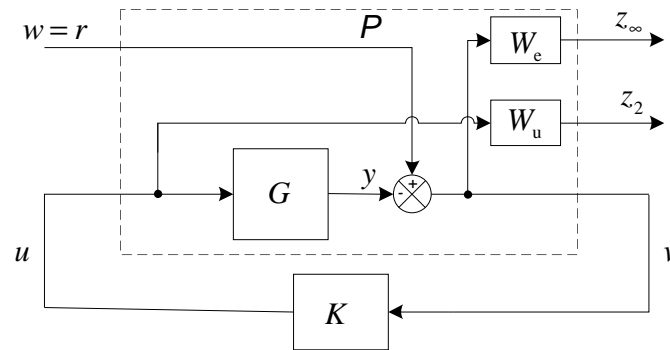


**Fig. 4.7:**  $S/KS$  mixed sensitivity optimization in standard form (tracking).

This work also considers other schemes, such as:

- $S/T$  (where the sensitivity function  $S$  is shaped by  $H_\infty$ -norm and  $T$  by  $H_2$ -norm)(Figure 4.8);
- $S/KS/KS$  (where one of the  $KS$  sensitivity functions are shaped by  $H_\infty$ -norm and second by  $H_2$ -norm) (Figure 4.9);
- $S/KS/T$  (where the sensitivity function  $S$  and the sensitivity function  $KS$  are shaped by  $H_\infty$ -norm and  $T$  by  $H_2$ -norm) (Figure 4.10);

- $S/T/KS$  (where the sensitivity function  $S$  and the complementary sensitivity function  $T$  are shaped by  $H_\infty$ -norm and  $KS$  by  $H_2$ -norm) (Figure 4.11);

Another useful mixed sensitivity optimization problem is to find a stabilizing controller which minimizes

$$\left\| \begin{bmatrix} W_e S \\ W_y T \end{bmatrix} \right\|_\infty \quad (4.5)$$

$T$  transfer function shaping is desirable for tracking problems and noise attenuation. It is also important for robust stability with respect to multiplicative perturbations at the plant output. The  $S/T$  mixed sensitivity minimization problem in the standard control configuration is presented below

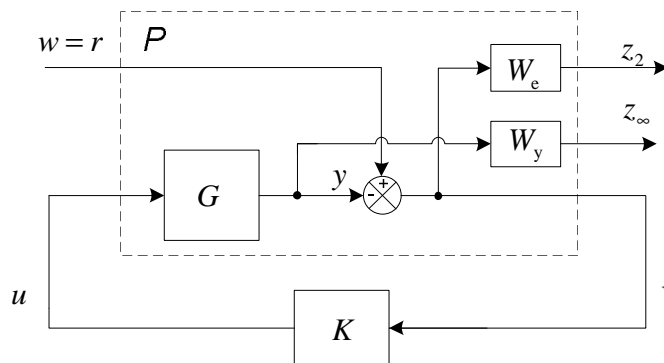


**Fig. 4.8:**  $S/T$  mixed sensitivity optimization in standard form.

All configurations mentioned above are used in standard mixed-sensitivity  $H_\infty$  optimization problems. But they also will be considered as the possible solutions of active magnetic bearing control problem.

It is known that the control cost can be more properly adjusted through  $H_2$  norm (Pal 2001). In accordance with this deduction  $H_2$  performance on controller output  $u$  at the design stage was added. The objective of this configuration (Figure 4.9) is to minimize

$$\left\| \begin{bmatrix} W_e S \\ W_{u1} K S \end{bmatrix} \right\|_{\infty} \quad \text{and} \quad \|[W_{u2} K S]\|_2 \quad (4.6)$$

The weighting function  $W_{u2}$  is used to compromise between the control effort and the disturbance rejection performance.

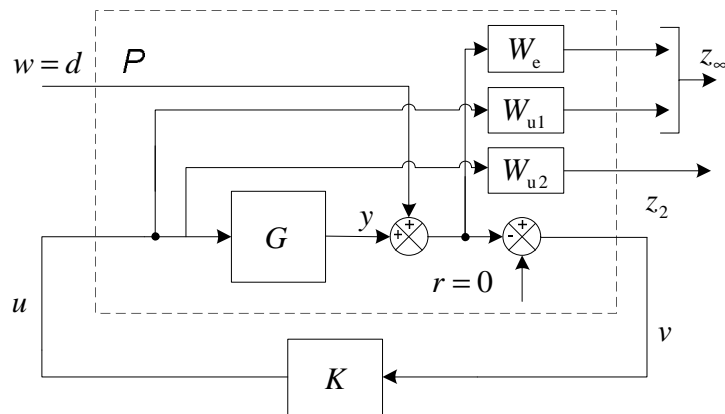


**Fig. 4.9:**  $S/KS - KS$  mixed sensitivity optimization.

Also  $S/KS - T$  (Figure 4.10) and  $S/T - KS$  (Figure 4.11) mixed sensitivity configurations are under consideration. In former one objective is to minimize output sensitivity and control signal transfer functions by  $H_{\infty}$  - norm and output complementary sensitivity transfer function by  $H_2$  - norm. In latter one the  $KS$  and  $T$  sensitivities are related to  $z_2$  and  $z_{\infty}$  outputs respectively. Recall that the  $H_{\infty}$  optimization responsible more for robustness of the system and  $H_2$  - for performance.

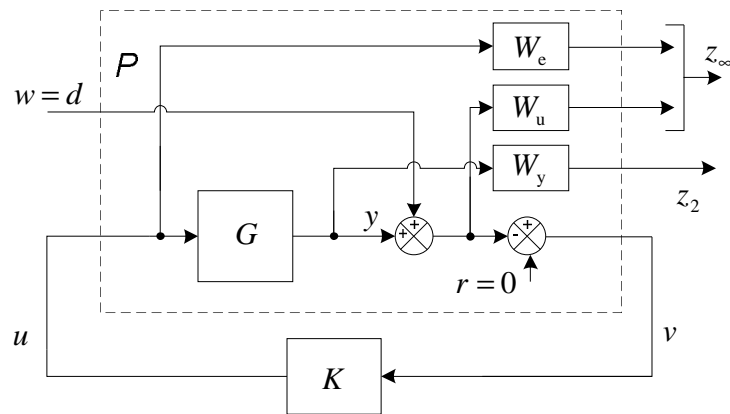


Fig. 4.10:  $S/KS - T$  mixed sensitivity optimization.

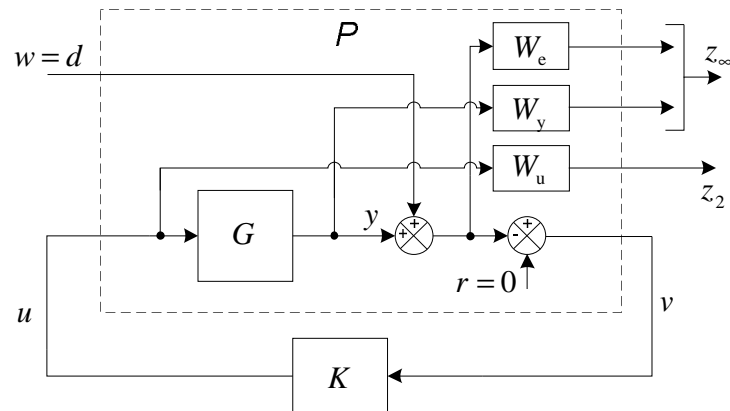


Fig. 4.11:  $S/T - KS$  mixed sensitivity optimization.

All these alternatives were used for controller designing and corresponding algorithms were written. The preliminary results were compared and according to them the scheme depicted in the Figure 4.9 was found to be the most convenient.

#### 4.1.2 Weighting functions

##### Performance weighting function.

The problem is to regulate the output  $y$  of the nominal plant to follow some given reference signal  $w$  and to reject the disturbance  $d$  by designing a controller  $K$ .

To improve the performance (to minimize the steady-state error) of the plant the following form of weighting function was suggested (Skogestad 2005):

$$W_e = \frac{s/M_e + \omega_e}{s + A_e \cdot \omega_e} . \quad (4.1)$$

It can be seen that at low frequencies  $|w_e(j\omega)|^{-1}$  is equal to  $A_e \leq 1$ , is equal to  $M_e \geq 1$  at high frequencies and the asymptote crosses 1 at the frequency  $\omega_e$ , which is approximately the bandwidth requirement.

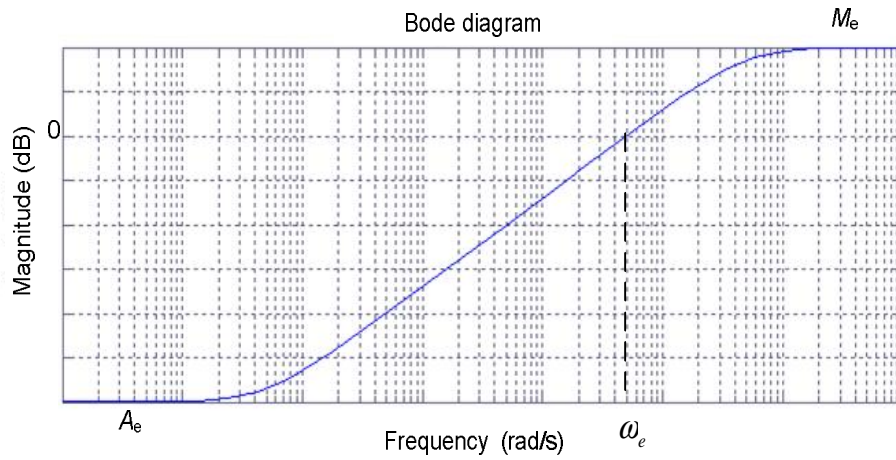


**Fig. 4.1:** Inverse of performance weight.

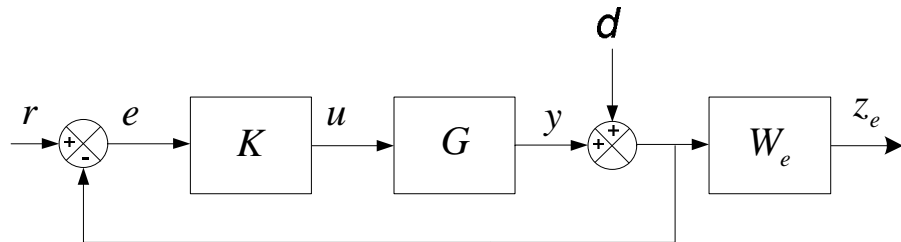


**Fig. 4.2:** Feedback system with output sensitivity weighting function.

By choosing an appropriate weighting function  $W_e$  the frequency response of  $S$  and the performance of the controlled system can be optimized, if the controller is designed such that the condition

$$\left| W_e(e^{j\omega T_s}) S(e^{j\omega T_s}) \right| < 1 \quad (4.2)$$

is holds.



### Control signal weighting function

Practically, an actuator always has amplitude and rate limit constraints. Hence, it is important to use a suitable weighting function to represent these constraints. In the case of  $KS$  sensitivity the same weighting function is considered as in performance optimization problem. Recall  $KS$  the transfer function between  $d$  and the control signals. So it is important to include  $KS$  to limit the size and bandwidth of the controller and hence the control energy used. The  $KS$  is also important for robust stability.

$$W_u = \frac{s / M_u + \omega_u}{s + A_u \cdot \omega_u} \quad (4.3)$$

But in previous problem the low-pass filter is needed, while here is high-pass filter to decrease the effect of external disturbances on control signal.

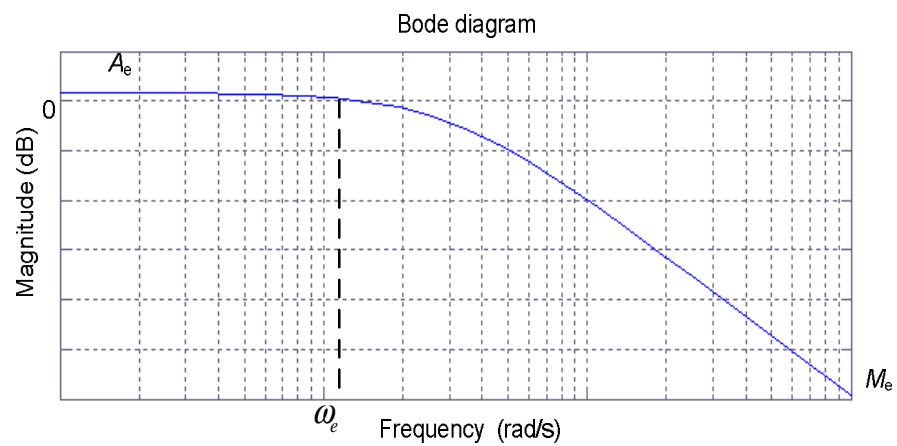


**Fig. 4.3:** Inverse of control signal weight.

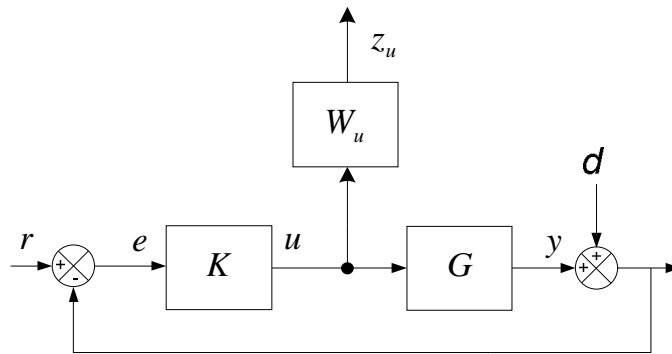


**Fig. 4.4:** Feedback system with output complementary sensitivity weighting function.

Also it would be considered the unity weighting function just to limit the magnitude of control signal, to keep it small of saving energy reason.

#### Complementary sensitivity weighting function

Optimizing system in case of complementary sensitivity  $T$  is good for tracking and reducing noise attenuation. Form of its weight as in two previous cases:

$$W_y = \frac{s/M_y + \omega_y}{s + A_y \cdot \omega_y} \quad (4.4)$$

It is also a high-pass filter like  $KS$ .

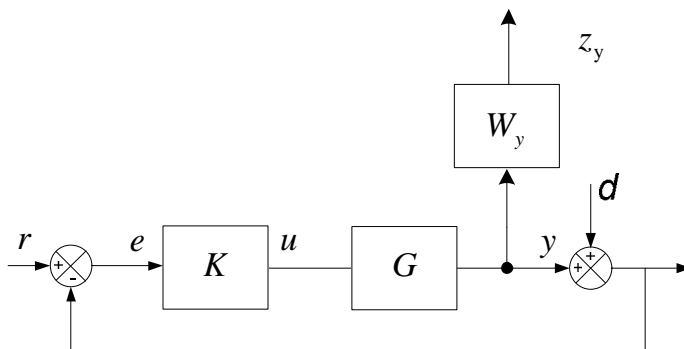


**Fig. 4.5:** Standard configuration of complementary sensitivity function  $T$  and weighting function.

To minimize error from  $r$  to  $e$ , or to suppress effect from interference  $w$ , the small sensitivity function  $S$  is better; while to keep object controlled robust stable, the small complementary function  $T$  is better. Therefore, there is an inevitable conflict between functions  $S$  and  $T$ . A compromise approach should be adopted. The ideal solution is to find the controller to separate  $S$  and  $T$  frequency domains, but it is hard to obtain this kind of controller.

As our problem is the multi-objective design problem the mixed sensitivity control would be the most relevant.

#### 4.2 Design procedure

The multi-objective design requirement can be formulated in the LMIs (Linear Matrix Inequality) framework and the controller is obtained by solving a family of LMIs (Skogestad 2005).

General mixed  $H_2/H_\infty$  control with pole placement scheme has multi-channel form as shown in Figure 4.12.  $P$  is a linear time invariant generalized plant;  $w = d$  is vector representing the disturbances or other exogenous input signals;  $z_\infty$  is the controlled output associated with  $H_\infty$  performance and  $z_2$  is the controlled output associated with  $H_2$  performance;  $u$  is the control input while  $y$  is the measured output.

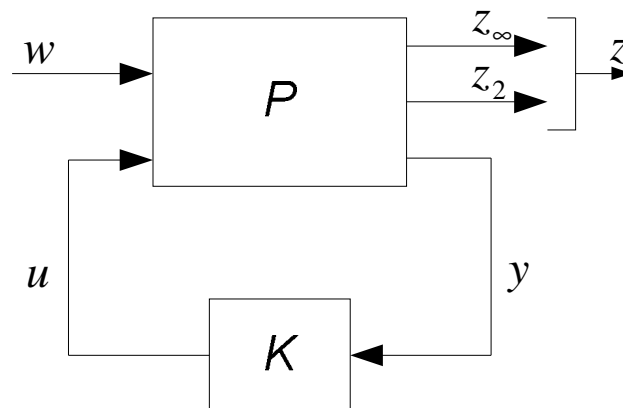


**Fig. 4.12:** Multi-objective synthesis.

The state-space description of above system can be written as:

$$\begin{aligned}
 \dot{\mathbf{x}} &= \mathbf{A}\mathbf{x} + \mathbf{B}_1\mathbf{w} + \mathbf{B}_2\mathbf{u} \\
 z_\infty &= \mathbf{C}_1\mathbf{x} + \mathbf{D}_{11}\mathbf{w} + \mathbf{D}_{12}\mathbf{u} \\
 z_2 &= \mathbf{C}_2\mathbf{x} + \mathbf{D}_{21}\mathbf{w} + \mathbf{D}_{22}\mathbf{u} \\
 \mathbf{y} &= \mathbf{C}_y\mathbf{x} + \mathbf{D}_y\mathbf{u}
 \end{aligned} \tag{4.7}$$

The goal is to compute an output-feedback controller  $K(s)$  in the form of

$$\begin{aligned}
 \zeta &= \mathbf{A}_K\zeta + \mathbf{B}_K\mathbf{y} \\
 \mathbf{u} &= \mathbf{C}_K\zeta + \mathbf{D}_K\mathbf{y}
 \end{aligned} \tag{4.8}$$

such that the closed-loop system meets mixed  $H_2/H_\infty$  specifications and pole placement constraint. This standard LMI problem is readily solved with LMI optimization software. An efficient algorithm for this problem is available in *hinfmix()* function of the LMI control toolbox for Matlab.

$$[\text{gopt}, h2opt, \mathbf{K}] = \text{hinfmix}(\mathbf{P}, \mathbf{r}, \text{obj}, \text{region}) \tag{4.9}$$

This function performs multi-objective output-feedback synthesis. *hinfmix* intend to compute an LTI controller  $K$  that minimizes the mixed  $H_2/H_\infty$  criterion

$$\alpha \|T_\infty\|_\infty^2 + \beta \|T_2\|_2^2 \tag{4.10}$$

subject to

- $\|T_\infty\|_\infty < \gamma_0$ ;
- $\|T_2\|_2 < \nu_0$ ;
- The closed-loop poles lie in some prescribed LMI region;

where  $T_\infty$  and  $T_2$  denote the closed-loop transfer functions from  $\omega$  to  $z_\infty$  and  $z_2$ , respectively (Balas 2009).

The function *hinfmix* returns guaranteed  $H_2$  and  $H_\infty$  performances *h2opt* and *gopt* as well as the matrix  $K$  of the LMI-optimal controller.

The input parameters of this function are generalized plant  $P$ ; three-entry vector  $r$ , which defines sizes of output  $z_2$ , output  $y$  and control signal  $u$ ; the four-entry vector **obj** =  $[\gamma_0, \nu_0, \alpha, \beta]$  specifies the  $H_2/H_\infty$  constraints and trade-off criterion (Petkov 2005).

Designing process of such controller consists of two main steps. The first one is to generate a suitable generalized plant, in other words to choose appropriate scheme, with weighting functions for each case mentioned in previous chapter. To achieve desirable characteristics, such as steady-state error, small magnitude of control signal, robustness, required performance, the correct weighting functions parameters should be selected on the second step.

In AMB system control the most important aim is to reject the output disturbances; in this context it is reasonable to use standard mixed-sensitivity framework ( $S/KS$ ):

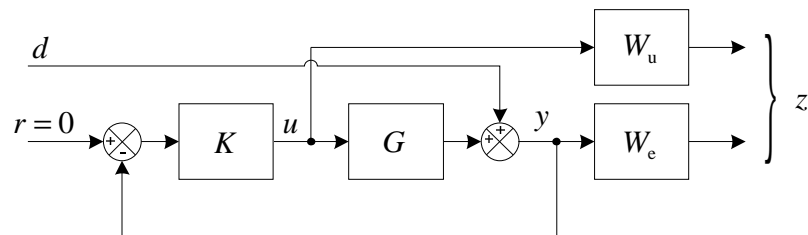


**Fig. 4.13:** Mixed-sensitivity output disturbance rejection.

Shaping the output sensitivity transfer function  $S$  and transfer function  $KS$  by weights  $W_e$  and  $W_u$  respectively, the inverse multiplicative uncertainty and additive uncertainty are also being optimized.

The  $H_2$  performance is considered for the controller output  $u$  (Figure 4.14):

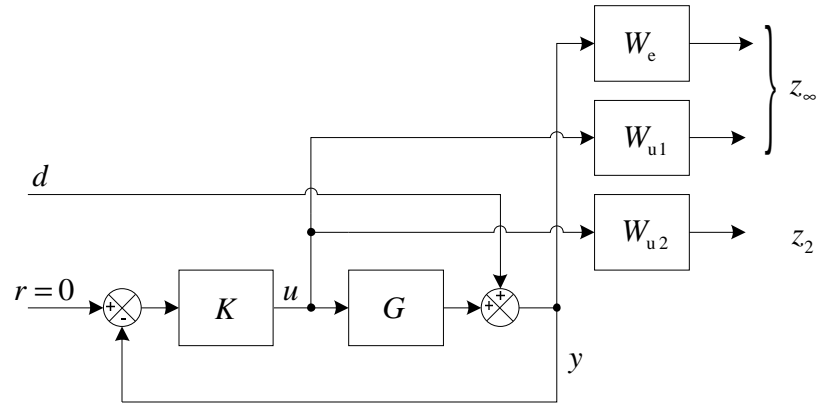


**Fig. 4.14:** Mixed-sensitivity output disturbance rejection with other constraints.

Using  $W_{u2}$  weight the high-pass filter could be done, and it will attenuate the high frequency influence from reference signal to control signal. So the desirable design scheme was achieved.

The generalized plant represented in the Figure 4.14 in mixed controller optimization problem used in form depicted in the Figure 4.12 and has two inputs and four outputs. The inputs are:

- $w$  : exogenous disturbance at the output of the plant;
- $u$  : control signal from controller;

The outputs are:

- $z_{\infty 1}$  : weighted by (4.11) and perturbed output of the plant (position of the rotor) (to  $H_{\infty}$ );
- $z_{\infty 2}$  : control signal (control current) (to  $H_{\infty}$ );
- $z_2$  : control signal (control current) (to  $H_2$ );
- $u(y)$  : not weighted, perturbed output of the plant (to controller).

After the generalized plant is constructed, the weighting functions should be tuned. It was done iteratively using *hinfmix()* in case when  $obj = [0 \ 0 \ 1 \ 1]$ .

Output sensitivity weight was fitted in such way to ensure the reduction of low-frequency disturbances 1000 times and unity amplification at high frequencies.

$$W_e = \frac{10^{-1}s + 11 \cdot 10^2}{s + 11 \cdot 10^2 \cdot 10^{-4}} = \frac{0.1s + 1100}{s + 0.11} . \quad (4.11)$$

Control signal weight optimized by  $H_\infty$ -norm minimization was selected as the unity (4.12), to guarantee the robustness. But for  $H_2$  optimization the high-pass filter is evaluated (4.13).

$$W_{u1} = \frac{s + 100}{s + 100} = 10^0 = 1 , \quad (4.12)$$

$$W_{u2} = \frac{s / (0.4 \cdot 10^{-3}) + 5 \cdot 10^5}{s + 10^0 \cdot 5 \cdot 10^5} = \frac{2500s + 5 \cdot 10^5}{s + 5 \cdot 10^5} . \quad (4.13)$$

But the relevant results were not achieved immediately. Initially was used standard weighting functions and further configured during the controller designing process.

When the parameters of weights are captured generalized plant could be generated and used as the input argument of function *hinfmix()* (4.9). At first the quadratic  $H_\infty$  performance subject to the pole placement constraint was computed by

$$gopt = \text{hinfmix}(\mathbf{P}, [1 \ 1 \ 1], [0 \ 0 \ 1 \ 0]); \quad (4.14)$$

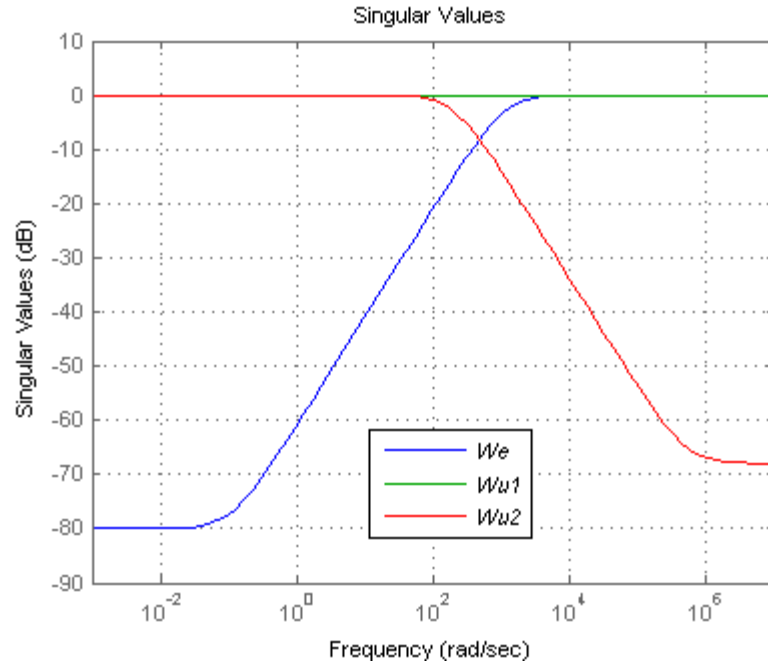


**Fig. 4.14:** Selected weights.

This algorithm yielded  $g_{opt} = 9.06$ . Suchwise the main aim is to keep this value as small as possible because of the disturbance rejection.  $g_{opt}$  specifies the peak value of the output sensitivity and complementary output sensitivity amplification.

Next the best  $H_2$  performance  $h2_{opt}$  subject to  $\|T_\infty\|_\infty < g_{opt}$  was computed by

$$[g_{opt}, h2_{opt}, \mathbf{K}] = \text{hinfmix}(\mathbf{P}, [1 \ 1 \ 1], [9.06 \ 0 \ 0 \ 1]); \quad (4.14)$$

But this determination became infeasible; it means that used function could not calculate the sufficient for required constraints controller. For this reason the  $g_{opt}$  was increased iteratively to  $g_{opt} = 10$ . At that point feasible solution  $h2_{opt} = 887$  was obtained.



The computed controller is

$$K = \frac{274.3s^5 + 1374 \cdot 10^5 s^4 + 119 \cdot 10^9 s^3 +}{s^6 + 7068s^5 + 238 \cdot 10^5 s^4 + 29 \cdot 10^9 s^3 +} \quad (4.12)$$

$$\frac{+ 2711 \cdot 10^{10} s^2 + 2232 \cdot 10^{12} s + 5731 \cdot 10^{13}}{+ 1828 \cdot 10^{10} s^2 + 1562 \cdot 10^{12} s + 1716 \cdot 10^{11}} .$$

The algorithm generating this controller is given in Appendix 1.

### 4.3 Results

To evaluate the features of the computed controller and closed-loop system it controls it is convenient to plot some responses and make simulations.

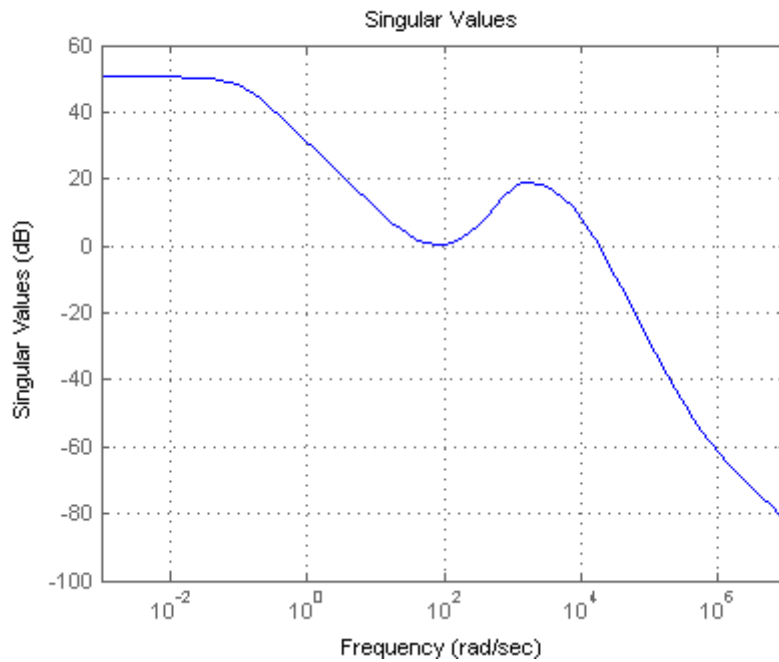


**Fig. 4.15:** Generated controller's singular value plot.

It can be seen in the Figure 4.15 that we succeeded in high-pass filtering the control signal, as the transfer function related to control signal is  $KS$ , where  $S$  has unity value at frequency 1370 rad/s (Figure 4.16).

Singular value plot (Figure 4.16) proves that we got tasks defined before:

- Low-pass filter for output disturbances (output sensitivity);
- High-pass filter for noise attenuation in control signal and measuring output.
- Closed-loop system is stable.

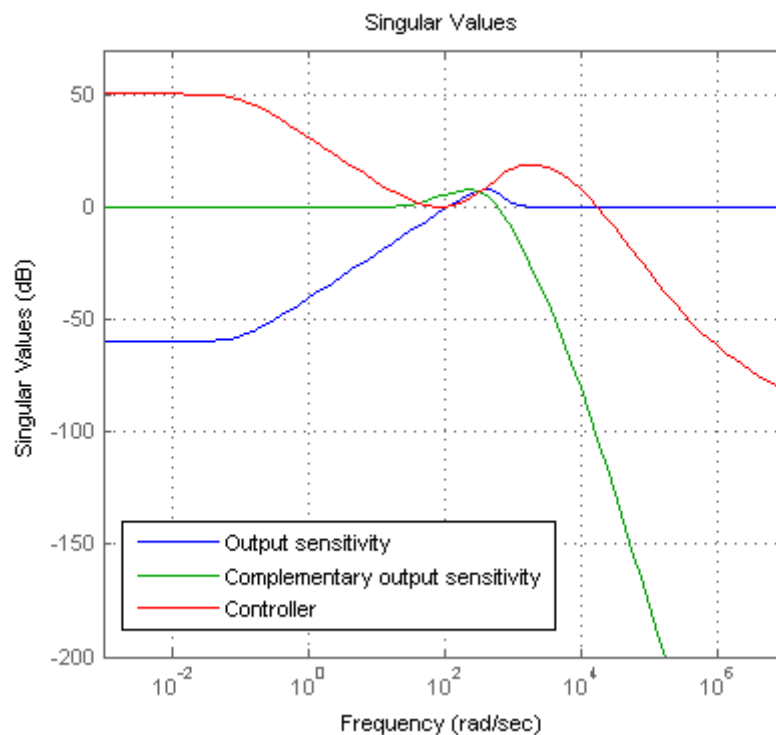


**Fig. 4.16:** Singular value plot of controller, closed-loop output sensitivity and complementary output sensitivity.

Poles and zeros of the closed-loop system with computed multi-objective controller are all located in left half plane, that arguing about stability of the system. All zeros and poles can be seen in the Figure 4.17, except one zero  $z = 5 \cdot 10^5$ .

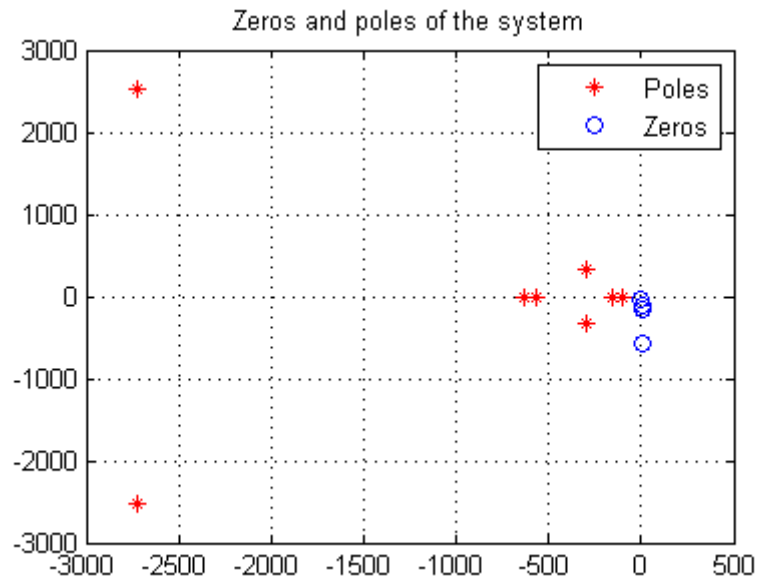


**Fig. 4.17:** Zeros and poles of closed-loop system.

Control signal makes a huge rise when the unity step signal fed on the input as a reference signal or on the output of the plant as the exogenous disturbance on the shaft. It goes without saying, that it is not good for the control system. So the saturation with limits [1;-1] was used to scale down this peak.

#### 4.3.1 Simulation

For descriptive reasons simulation model of closed-loop system was created using Simulink, including Robust Control Toolbox™ blocks.

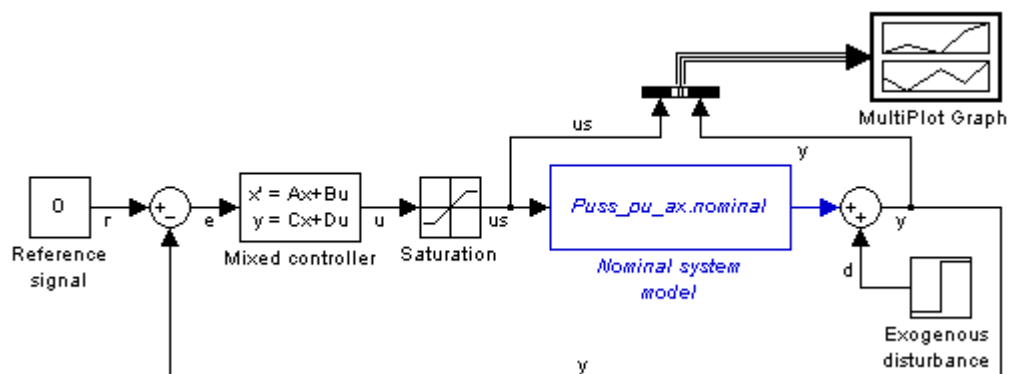


**Fig. 4.18:** Simulation with nominal model.

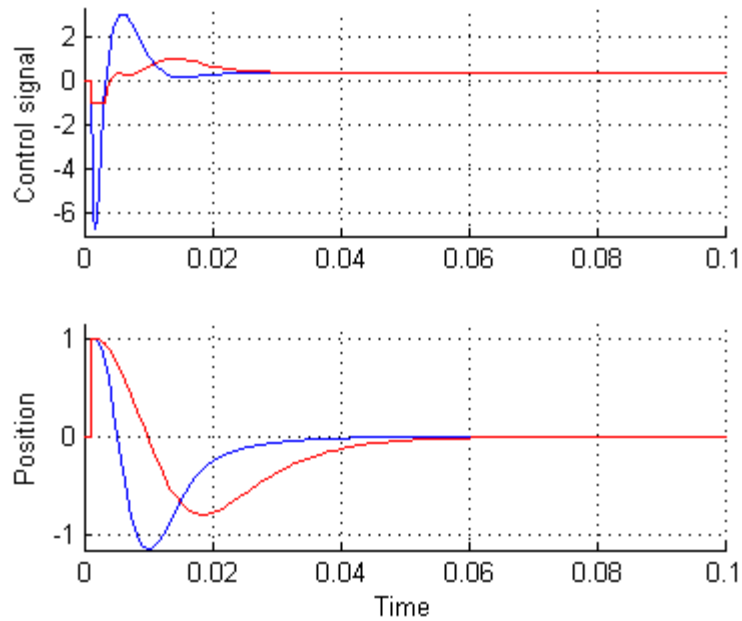


**Fig. 4.19:** Closed-loop nominal system step responses on the output of the plant (exogenous disturbance): with saturation (red) and without (blue).

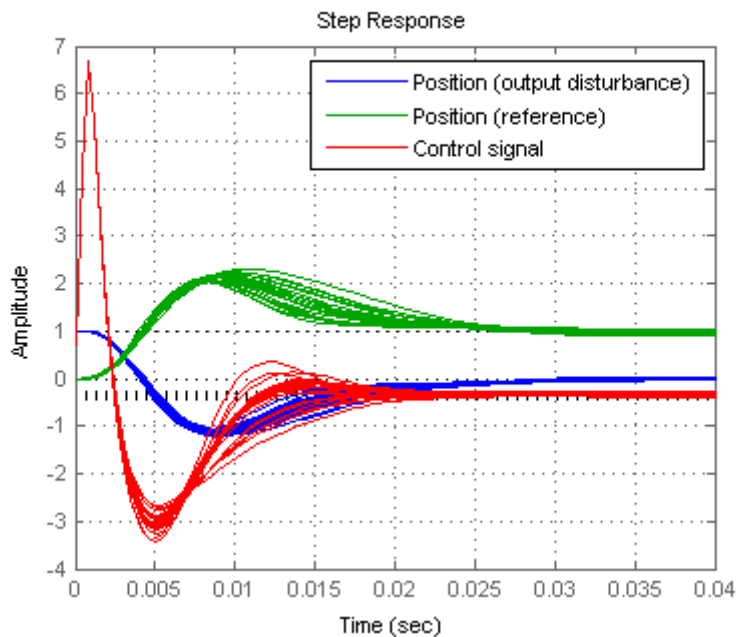


**Fig. 4.20:** Closed-loop uncertain system step responses.

Figure 4.20 illustrates the system behavior when some parameters have the uncertainties. For the one-degree-of-freedom controller designing results are satisfactory. But there is one more very important objective – the robustness of

the system to uncertainties. To check this feature the simulation with uncertainty model of axial bearings was done. Scheme for this simulation is the same as for nominal, but the special block from Simulink Robust Toolbox was used to import uncertain system model (Jastrzebski 2007). It is called USS System. The corresponding plots are shown in the Figure 4.20.

#### 4.3.2 Robust stability check

Robust stability of the closed-loop uncertain system could be checked with the function *robuststab()*:

$$[stabmarg, desgtabu, report, info] = robuststab(sys) \quad (4.13)$$

It returns the structure *stabmarg* with the following fields

Table 3. *Stabmarg* fields description.

Field	Description
<i>LowerBound</i>	Lower bound on stability margin, positive scalar. If greater than 1, then the uncertain system is guaranteed stable for all values of the modeled uncertainty. If the nominal value of the uncertain system is unstable, then <i>stabmarg.UpperBound</i> and <i>stabmarg.LowerBound</i> will be infinite.
<i>UpperBound</i>	Upper bound on stability margin, positive scalar. If less than 1, the uncertain system is not stable for all values of the modeled uncertainty.
<i>DestabilizingFrequency</i>	The critical value of frequency at which instability occurs, with uncertain elements closest to their nominal values. At a particular value of uncertain elements, the poles migrate across the stability boundary (imaginary-axis in continuous-time systems, unit-disk in discrete-time systems) at the frequency given by <i>DestabilizingFrequency</i> (Balas 2009).

If the robust stability margin exceeds 1, the uncertain system is stable for all values of its modeled uncertainty. And inversely, if stability robustness margin

is less than 1, the certain allowable values of the uncertain elements, within their specified ranges, lead to instability (Balas 2009). And so we get

$$\begin{aligned} UpperBound &= 9.9046 \\ LowerBound &= 2.5937 \\ DestabilizingFrequency &= 423.5236 \end{aligned} \quad (4.14)$$

Structure of values of uncertain elements which cause instability:

$$\begin{aligned} \omega_{bw} &= 271.2160 \\ k_i &= 218.1180 \\ k_x &= -7.1158 \cdot 10^5 \\ m &= 38.4642 \\ senon &= 1.2587 \end{aligned} \quad (4.15)$$

Stability robustness margins are greater than 1, hence the uncertain system is robustly stable to modeled uncertainty. The third output argument *report* gives some description of robustness analysis results:

- It can tolerate up to 259% of the modeled uncertainty.
- A destabilizing combination of 990% of the modeled uncertainty exists, causing instability at 424 rad/s.

Also it gives the information about sensitivity with respect to uncertain element:

- 'Wbw' is 3%. Increasing 'Wbw' by 25% leads to a 1% decrease in the margin.
- 'ki' is 44%. Increasing 'ki' by 25% leads to an 11% decrease in the margin.
- 'kx' is 33%. Increasing 'kx' by 25% leads to an 8% decrease in the margin.

- 'm' is 2%. Increasing 'm' by 25% leads to a 1% decrease in the margin.
- 'sennon' is 17%. Increasing 'sennon' by 25% leads to a 4% decrease in the margin.

So we can make a conclusion that obtained system is stable for parameters uncertainties and exogenous disturbances.

Functions *robuststab()* and *robustperf()* (used in the next chapter for robust performance analysis) also provides  $\mu$ -analysis, in which the stability margin should not be greater than 1 to guarantee the robust stability (Skogestag).

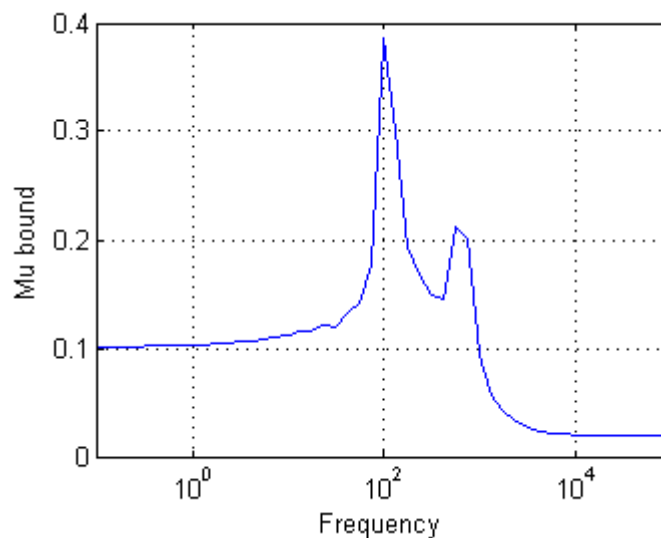


**Fig. 4.21:**  $\mu$  plot of robust stability margin.

As shown in the Figure 4.21 the  $\mu$  bound is less than 1 that verifies the closed-loop uncertain system robust stability for prescribed parameters uncertainties.

#### 4.3.3 Robust performance check

The performance of the nominally stable system could degrade for some values of uncertain parameters. Upon this fact it is reasonable to define the robust

performance margins. With this end in view it is convenient to use the function *robustperf()* from Robust Control Toolbox™:

$$[perfmarg,perfmargunc,report] = \text{robustperf}(sys) \quad (4.16)$$

It returns the structure *perfmarg* with the following fields

Table 4. *Perfmarg* fields description.

Field	Description
<i>LowerBound</i>	Lower bound on robust performance margin, positive scalar.
<i>UpperBound</i>	Upper bound on robust performance margin, positive scalar.
<i>CriticalFrequency</i>	The value of frequency at which the performance degradation curve crosses the $y=1/x$ curve. See "Generalized Robustness Analysis" in the online documentation (Balas 2009).

And for uncertain system model of AMBs we get:

$$\begin{aligned} UpperBound &= 0.3683 \\ LowerBound &= 0.3573 \\ CriticalFrequency &= 423.5236 \end{aligned} \quad (4.17)$$

The margin 0.3683 means that for all values of uncertain elements which are less than 0.3683 normalized units away from their nominal values, the input/output gain remains less than  $1/0.3683 = 2.715 \approx 2.8$ . *CriticalFrequency* is a Frequency at which the minimum robust performance margin occurs.

Structure of values of uncertain elements which cause critical influence on performance robustness:



$$\begin{aligned}
 \omega_{bw} &= 555.5775 \\
 k_i &= 220.9331 \\
 k_x &= 9.8694 \cdot 10^5 \\
 m &= 46.3118 \\
 sennon &= 1.0184
 \end{aligned}
 \tag{4.18}$$

As for the robust stability here is the information from the function argument *report* about robust performance (margin is 0.3683):

- A model uncertainty exists of size 35.7% resulting in a performance margin of 2.8 at 424 rad/sec.

Sensitivity with respect to uncertain element is:

- 'Wbw' is 2%. Increasing 'Wbw' by 25% leads to a 1% decrease in the margin.
- 'ki' is 8%. Increasing 'ki' by 25% leads to a 2% decrease in the margin.
- 'kx' is 2%. Increasing 'kx' by 25% leads to a 1% decrease in the margin.
- 'm' is 1%. Increasing 'm' by 25% leads to a 0% decrease in the margin.
- 'sennon' is 2%. Increasing 'sennon' by 25% leads to a 1% decrease in the margin.

The structured singular value ( $\mu$ ) is the reciprocal of the performance margin.

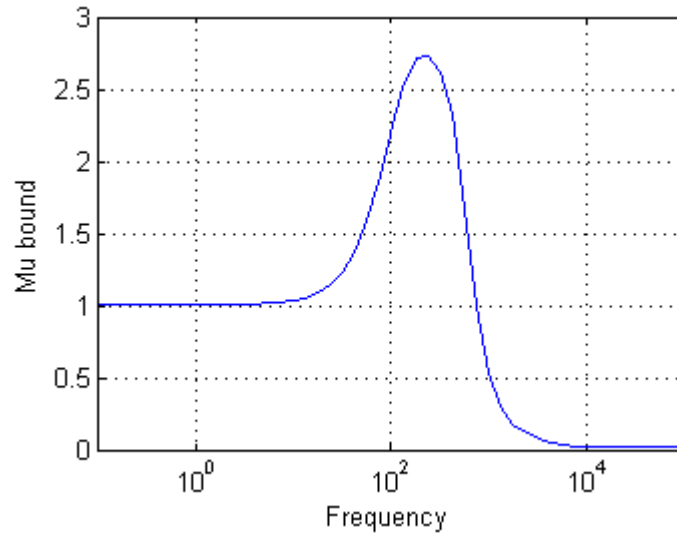


**Fig. 4.22:**  $\mu$  plot of robust performance bound.

Figure 4.22 shows that the achieved robust performance is not as good as it required for AMB rotor system, the better results can be achieved by adding a second degree of freedom for the controller.

Summarizing it could be said that 1DOF mixed  $H_2/H_\infty$  robust controller have been designed. Obtained controller is stable and has good performance, but if we want to evaluate it is necessary to compare it to any other controller. For example, mixed controller compared to the  $H_\infty$  controller in the next chapter.

#### 4.4 Comparison of mixed $H_2/H_\infty$ and $H_\infty$ controllers

As a part of the work the  $H_\infty$  robust controller was designed to be compared with mixed controller. This was done to assess the relevance of the work and to determine the direction of future work in this area. The algorithm of computing  $H_\infty$  controller is represented in the Appendix 2.

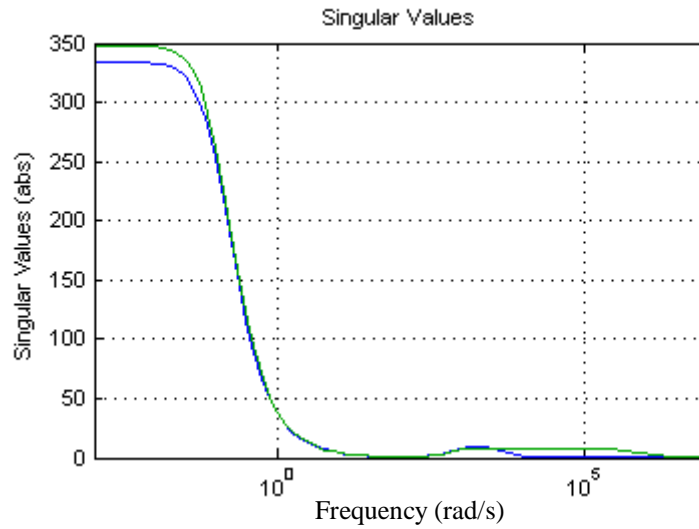
The comparative characteristics of robustness of the systems are represented in Table 5. Controllers were compared in two cases: when the output sensitivities transfer functions have equal bandwidths ( $\omega_b = 80(\text{rad/s})$ ) and equal peaks (8.3 dB). Such a decision was made according to the fact that it is impossible to get the identical output sensitivities.

Table 5. Comparative characteristics

Controller \ Parameter		Robust stability		Robust performance	
		Upper bound	Lower bound	Upper bound	Lower bound
Equal bandwidths ( $\omega_b = 80(\text{rad/s})$ )	$H_2/H_\infty$	9.9046	2.5937	0.3683	0.3573
	$H_\infty$	8.6025	2.5433	0.4133	0.4019
Equal peaks (8.3 dB).	$H_2/H_\infty$	9.9046	2.5937	0.3683	0.3573
	$H_\infty$	10	2.2210	0.3052	0.3083

By reference to derived data, can be drawn the conclusions that the closed-loop system with mixed controller has a higher stability margins than the system with  $H_\infty$  controller in equal bandwidth condition, that implies more robust system. It is quite good, but the performance margins are better in  $H_\infty$  case. The situation is opposite in equal peaks condition. But the degradation in robust stability margins is not so significant as the improvement of performance margins. Numerically, stability margins are 1% lower, as the performance margins are 18% greater.

There are also advantages of mixed controller in the reference signal noise attenuation (Figure 4.24), tracking (Figure 4.24) and control signal high frequency noise filtering (Figure 4.23). This can be seen in the figures below.



**Fig. 4.23:** Singular value plots of mixed (blue) and  $H_\infty$  (green) controllers.

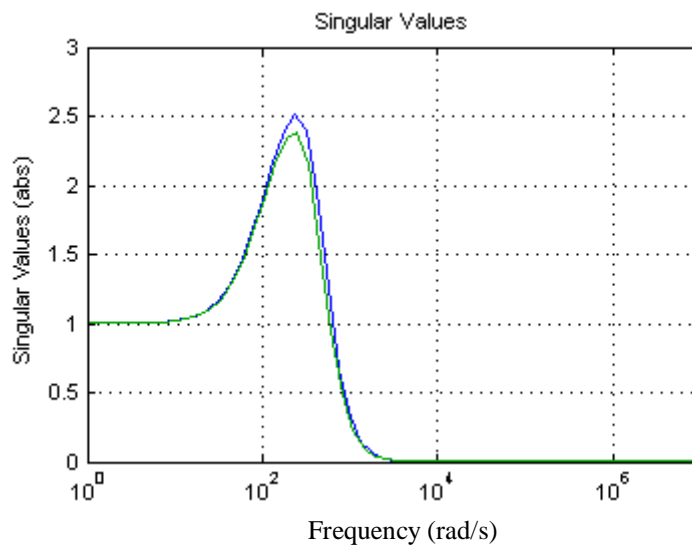


**Fig. 4.24:** Singular value plots of the output complementary sensitivities of closed-loop systems controlled by  $H_2/H_\infty$  (blue) controller and  $H_\infty$  (green).

As a result the one-degree-of-freedom mixed  $H_2/H_\infty$  robust controller was designed. The robustness of the AMB system controlled by such controller is guaranteed. The overshoots of signal and position are too high for real system. But in spite of that the controller has only one DOF the axial bearing system model controlled by it has satisfactory robust characteristics. By adding the second degree of freedom to obtained controller the time domain characteristics can be met.

## 5 Conclusions

A lot of control methods are available at the present time to control the objects of all kinds. Hence there are also many design techniques for their implementation. In this work the object is the model of axial active magnetic bearings. Robust control method was considered to achieve the formulated problems including the improvement of the system robustness, performance, stability, output disturbance rejection and noise attenuation.

To implement the controller with which the closed-loop system will satisfy the requirements the mixed  $H_2/H_\infty$  optimization was chosen in this thesis. This way the outputs norms of generalized plant are minimized by  $H_2$  and  $H_\infty$  norms. To shape the required transfer functions, as output sensitivity ( $S_o = (I + GK)^{-1}$ ), complementary output sensitivity ( $T_o = GK(I + GK)^{-1}$ ), from reference signal to control signal ( $R = K(I + GK)^{-1}$ ) the weighting functions in form of low-pass and high-pass filtering were used. The generalized plant was generated in such a way to minimize the second norm of weighted  $R$  and the infinity norms of weighted  $R$  and  $S$ . The design process was realized using Robust Control Toolbox™ of the MATLAB. Especially to compute the controller used function *hinfmix()*. Therefore the required mixed  $H_2/H_\infty$  controller has been designed.

To see the relevance of this direction of working controller was compared with  $H_\infty$  optimization approach. The comparison results are not allowing adjudicating upon the indisputable dominance of mixed controller but it has better properties than simple  $H_\infty$ .

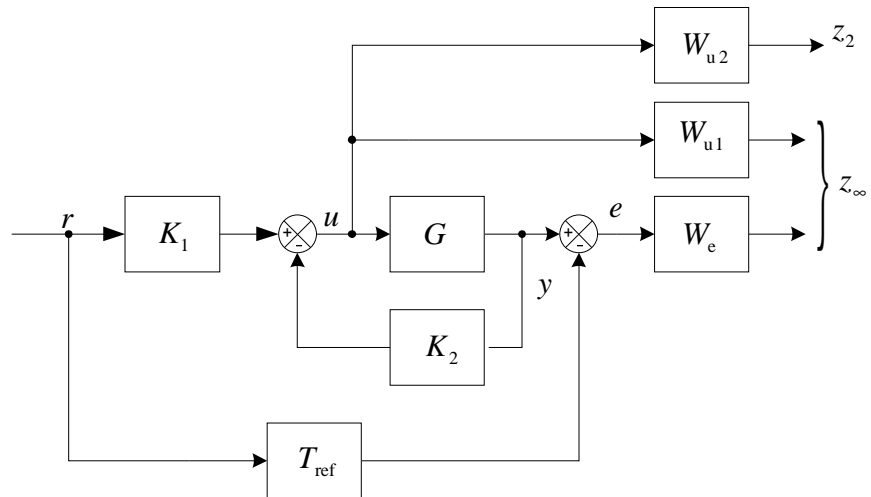


**Fig. 5.1:** Two degree-of-freedom controller scheme ( $T_{\text{ref}}$  - reference model).

One degree-of-freedom controller configuration was considered. Even that way the derived closed-loop system has quite good performance and stability characteristics. Deficiencies of system can be disposed by appending the second degree-of-freedom to controller. The principle of a 2DOF control scheme is to use a feedback controller ( $K_2$ ) to achieve the internal and robust stability, disturbance rejection, *etc.*, and to design another controller ( $K_1$ ) on the feed forward path to satisfy the tracking requirement, which minimizes the difference between the output of the system and reference signal. The structure of such control is shown in the Figure 5.1. For the future such controller properties can be investigated more detailed and trying this optimization for radial bearings as well.

## References

- Akhtar J. and Uddin V. *Trade-off between the  $H_2$  and  $H_\infty$  in the multi-objective state feedback synthesis through LMI characterizations*. Pakistan Navy Engineering College (PNEC), National University of Sciences & Technology (NUST).
- Athuts M. 1971. *The role and use of the stochastic linear-quadratic-Gaussian problem in control system design*. IEEE transactions on automatic control, vol. ac-16, n o. 6.
- Balas G., Chiang R., Packard A., Safonov M. 2009. *Robust Control Toolbox™ User's Guide*.
- Besekersky V.A., Popov E.P. 2004. *Теория систем автоматического регулирования (Theory of automatic control systems)*. Professija, Saint-Petersburg, Russia.
- Chen H. 2006. *Wide-area Robust  $H_2/H_\infty$  Control with pole placement for Damping Inter-area Oscillations*. Power Engineering Society General Meeting, IEEE.
- Coonick A.H., Pal B.C., Cory B.J. 2001. *Robust pole placements versus root-locus approach in the context of damping inter area oscillations in power systems*. Generation, Transmission and Distribution, IEE Proceedings- Volume 149, Issue 6, Nov. 2002 Page(s):739 – 745
- Damen A., Weiland S. 2002. *Robust Control*. Eindhoven University of Technology. Set of lectures. <http://www.ee.pucrs.br/~gacs/new/disciplinas/ppgee/crobusto/referencias/nates.pdf>

- Egurov N.D., Pupkov K.A. 2004. *Методы классической и современной теории автоматического управления. Учебник в 5 томах. Том 3. Синтез регуляторов систем автоматического управления (Methods of classical and modern theory of automatic control. Tome 3: Synthesis of Regulators of automatic control systems)*. Moscow State Technical University n.a. N.E. Bauman (MSTU).
- Gahinet P., et al. 1995. *LMI Control Toolbox User's Guide*. The MathWorks, Inc.
- Jastrzebski R.P. 2007. *Design and implementation of FPGA-based LQ control of active magnetic bearings*. Lappeenranta University of Technology, Finland, Lappeenranta.
- Kwakernaak H. 1972. *Linear Optimal Control Systems*. Wiley-Interscience, A Division of John Wiley & Sons Inc., N.Y.-London-Sydney-Toronto.
- Miroshnik I.V., Nikiforov V.O., Fradkov A.L. 2000. *Нелинейное и адаптивное управление в сложных динамических системах. (Nonlinear and adaptive control of complicated dynamic systems)*. Nauka, Saint-Petersburg, Russia (line: Analyze and synthesis nonlinear systems).
- Petkov P. H., Konstantinov M. M. 2005. *Robust control design with MatLab*. Springer-Verlag London ltd., England, London.
- Rollins L. 1999. *Robust Control Theory (18-849b Dependable Embedded Systems)*. Carnegie Mellon University. [Available online at [ece.cmu.edu/~koopman/des\\_s99/control\\_theory/](http://ece.cmu.edu/~koopman/des_s99/control_theory/)]
- Skogestad S., Postlethwaite I. 2005. *Multivariable feedback control - Analysis and design*. 2nd Edition, Wiley.



Thang M.T. 2002. *Robust stability and robust performance*. Part of a set of lecture notes on Introduction to Robust Control. [Available online at [lorien.ncl.ac.uk/ming/robust/robust.pdf](http://lorien.ncl.ac.uk/ming/robust/robust.pdf)]

Toivonen H. *Robust stability and the  $H_\infty$  norm*. Ebo Academy University. [Available online at [web.abo.fi/~htoivone/courses/robust/rob5.pdf](http://web.abo.fi/~htoivone/courses/robust/rob5.pdf)]

Zhao X., et al. 2006. *Robust  $H_2$  Control with Adaptive Mechanism*. Proceedings of the IEEE ,International Conference on Robotics and Biomimetics, December 17 - 20, 2006, Kunming, China

Mixed  $H_2/H_\infty$  controller computation algorithm.

```

clear all; load plants.mat; clc;
%% Input parameters: output weighting function Wp
Gnom = Puss_pu_ax.nominal; % Nominal plant model
Gunc = Puss_pu_ax; % Uncertain plant model

% S = (I+GK)^-1 - weighting function We for Hinf optimization
Ke0 = 1e-4; Ke8 = 1e0; we = 11e2;
We = tf([1/Ke8 we],[1 we*Ke0]);
% R = K(I+GK)^-1 - weighting function Wul for Hinf optimization
Ku10 = 1e0; Ku18 = 1e0; wu1 = 1e2;
Wu1 = tf([1/Ku18 wu1],[1 wu1*Ku10]);

% R = K(I+GK)^-1 - weighting function Wu2 for H2 optimization
Ku20 = 1e0; Ku28 = 0.4e-3; wu2 = 5e5;
Wu2 = tf([1/Ku28 wu2],[1 wu2*Ku20]);

%% Generalized plant P with weighting functions

systemnames = 'Gnom We Wu1 Wu2';
inputvar = '[r;u]';
outputvar = '[We;Wu1;Wu2;r-Gnom]';
input_to_Gnom = '[u]';
input_to_Wu1 = '[u]';
input_to_Wu2 = '[u]';
input_to_We = '[r-Gnom]';
sysoutname = 'P';
cleanupsysic = 'yes';
sysic;
P1 = ltisys(P.a,P.b,P.c,P.d);

%% Mixed H2/Hinf Controller design
[Gnompt,h2opt,Kmxd] = hinfmix(P1,[1 1 1],[10 0 0 1]);

%% Some transformations
[a,b,c,d] = ltiss(Kmxd); Kssmxd = ss(a,b,c,d);

% Nominal model
% Sensitivity functions of plant-controller feedback loop
loops = loopsens(Gnom*Kssmxd,1);
% Closed-loop state-space model
CL = feedback(Gnom*Kssmxd,1);
% Closed-loop LTI model
CLt = ltisys(CL.a,CL.b,CL.c,CL.d);
% Closed-loop with control signal as output
Fu = feedback(Kssmxd,Gnom);

% Model with uncertainties
% Sensitivity functions of plant-controller feedback loop
lpus = loopsens(Puss_pu_ax*Kssmxd,1);
% Closed-loop state-space model
CLus = feedback(Puss_pu_ax*Kssmxd,1);

```

```

% Closed-loop LTI model
CLtus = ltisys(CL.a,CL.b,CL.c,CL.d);
% Closed-loop with control signal as output
Fuus = feedback(Kssmxd,Puss_pu_ax);

% Zeros and poles of the nominal model
Ps = pole(CL);
Zs = zero(CL);
Zs1 = Zs(2:5);

%% Responses
figure(1); sigma(1/We,loops.So,loops.To); grid on; hold on;
figure(1); Legend('Weight S', 'Output sensitivity', 'Output
complementary sensitivity', 'Location', 'SouthWest');

figure(2); step(loops.So,CL,Fu); grid on; hold on
figure(2); legend('Output sensitivity', 'Closed loop', 'Control
signal');

figure(3); impulse(loops.So,loops.To); grid on; hold on
figure(3); Legend('Output sensitivity', 'Output complementary
sensitivity');

figure(4); plot(Ps, '*r'); hold on; grid on;
           plot(Zs1, 'ob');
title('Zeros and poles of the system');

figure(5); sigma(1/We,lpus.So,lpus.To); grid on; hold on;
figure(5); Legend('Weight S', 'Output sensitivity', 'Output
complementary sensitivity', 'Location', 'SouthWest');

figure(6); step(lpus.So,CLus,Fuus); grid on; hold on
figure(6); legend('Output sensitivity', 'Closed loop', 'Control
signal');

```

$H_\infty$  controller computation algorithm.

```

clear all; load plants.mat; clc;
%% Input parameters: output weighting function We
Go = Puss_pu_ax.nominal; % Nominal plant model

% S = (I+GK)^-1 - weighting function We
Ke0 = 1.144e-4;      Ke8 = 1e0;      we = 9.6e2;
We = tf([1/Ke8 we],[1 we*Ke0]);

% R = K(I+GK)^-1 - weighting function Wu1 for Hinf optimization
Ku0 = 1e0;      Ku8 = 1e-3;      wu = 6e6;
Wu = tf([1/Ku8 wu],[1 wu*Ku0]);

%% H8 mixed-sensitivity synthesis (S/T)
clc;
[K,CL,gam,INFO]=mixsyn(Go,We,Wu,[],'display','on');
%% Some transformations

% Sensitivity functions of plant-controller feedback loop
loops = loopsens(Go*K,1);
% Closed-loop state-space model
CL = feedback(Go*K,1);
% Closed-loop LTI model
CLt = ltisys(CL.a,CL.b,CL.c,CL.d);
% Closed-loop with control signal as output
Fu = feedback(K,Go);

%% Responses
figure(1); sigma(1/We,loops.So,loops.To); grid on; hold on;
figure(1); Legend('Weight S','Output sensitivity','Output
complementary sensitivity','Location','SouthWest');

figure(2); step(loops.So,CL,Fu); grid on; hold on
figure(2); legend('Output sensitivity','Closed loop','Control
signal');

figure(3);impulse(loops.So,loops.To); grid on; hold on
figure(3);Legend('Output sensitivity','Output complementary
sensitivity');

figure(4);plot(spol(CLt),'+b'); grid on;
title('Poles of the system');

```

$H_\infty$  and mixed  $H_2/H_\infty$  controller comparison computation algorithm.

```

clear all; clc; close all; load plants.mat;
%% Mode selection: 1 - Equal bandwidth; 2 - Equal peaks
disp(sprintf('\nBecause of the fact, that the output
sensitivities in Hinf \nand H2/Hinf optimizations can not be
equal at a time we \nshould choose what would be equal:\n'));
    disp('1) Equal bandwidth');
    disp('2) Equal peaks');
    choice=input('choice: ');

%% Output and control signal weighting functions for Hinf/H2
optimization.
Gnom = Puss_pu_ax.nominal;
% ax_plant; % Given plant
Gunc = Puss_pu_ax;

% S = (I+GK)^-1 - weghting function We
Ke0 = 1e-4;      Ke8 = 1e0;      we = 11e2;
Wemxd = tf([1/Ke8 we],[1 we*Ke0]);

% R = K(I+GK)^-1 - weghting function Wul for Hinf optimization
Ku10 = 1e0;      Ku18 = 1e0;      wu1 = 1e2;
Wumxd1 = tf([1/Ku18 wu1],[1 wu1*Ku10]);

% R = K(I+GK)^-1 - weghting function Wu2 for H2 optimization
Ku20 = 1e0;      Ku28 = 0.4e-3;      wu2 = 5e5;
Wumxd2 = tf([1/Ku28 wu2],[1 wu2*Ku20]);

%% Output and control signal weighting functions for Hinf
optimization.

% S = (I+GK)^-1 - weghting function We
if choice == 1
    % Bandwidths and low frequency gain are equal
    Le0 = 1.144e-4;      Le8 = 1.279e0;      we = 9.62e2;
else
    % Peaks and low frequency gain are equal
    Le0 = 2.91838e-4;      Le8 = 1.279e0;      we = 1e2;
end

Weinf = tf([1/Le8 we],[1 we*Le0]);

% R = K(I+GK)^-1 - weghting function Wul for Hinf optimization
Lu0 = 1e0;      Lu8 = 1e0;      wu = 1e2;
Wuinf = tf([1/Lu8 wu],[1 wu*Lu0]);

```

## Appendix III, 2

```

%% Generalized plant P for Hinf/H2 optimization.
clc;
systemnames      = 'Gnom Wemxd Wumxd1 Wumxd2';
inputvar         = '[r;u]';
outputvar        = '[Wemxd;Wumxd1;Wumxd2;r-Gnom]';
input_to_Gnom    = '[u]';
input_to_Wumxd1 = '[u]';
input_to_Wumxd2 = '[u]';
input_to_Wemxd   = '[r-Gnom]';
sysoutname       = 'P';
cleanupsysic     = 'yes';
sysic;
P1 = ltisys(P.a,P.b,P.c,P.d);

%% Mixed H2/Hinf Controller design
[Gnompt,h2opt,Kmxd] = hinfmix(P1,[1 1 1],[10 0 0 1]);

%% H8 mixed-sensitivity synthesis (S/R)
[Kinf,CL,gam,INFO]=mixsyn(Gnom,Weinf,Wuinf,[],'display','on');

%% Some transformations
disp(sprintf('\nPress any key to see the responses\n'));
pause ;
clc;
disp(sprintf('\nSelect the plant\n'));
    disp('1) Nominal');
    disp('2) Uncertaint');
plant=input('choice: ');
    if plant == 2
        Gnom = Gunc;
    end
[a,b,c,d] = ltiss(Kmxd); Kssmxd = ss(a,b,c,d);

% Hinf                                     % Hinf/H2
% Sensitivity functions of plant-controller feedback loop
lpinf = loopsens(Gnom*Kinf,1);              lpmxd =
loopsens(Gnom*Kssmxd,1);

% Closed-loop state-space model
CLinf = feedback(Gnom*Kinf,1);              CLmxd =
feedback(Gnom*Kssmxd,1);

% Closed-loop with control signal as output
Fuinf = feedback(Kinf,Gnom);                Fumxd =
feedback(Kssmxd,Gnom);

OutputSens_Mxd = lpmxd.So;
OutputSens_Hinf = lpinf.So;
COutputSens_Mxd = lpmxd.To;
COutputSens_Hinf = lpinf.To;
% Poles
PLmxd = spol(CLtmxd);
PLinf = spol(CLtinf);

```

## Appendix III, 3

```

%% Responses
figure(1);
sigma(OutputSens_Mxd,OutputSens_Hinf,COutputSens_Mxd,COutputSens
_Hinf,Kssmxd,Kinf); grid on; hold on;
figure(1); Legend('Output sensitivity(mixed)', 'Output
sensitivity(Hinf)', 'Output complementary
sensitivity(mixed)', 'Output complementary
sensitivity(Hinf)', 'Kssmxd', 'Kinf', 'location', 'SouthWest');

figure(2); step(OutputSens_Mxd,OutputSens_Hinf,Fumxd,Fuinf,0:1e-
6:0.04); grid on; hold on
figure(2); legend('Output sensitivity(mixed)', 'Output
sensitivity(Hinf)', 'Output complementary
sensitivity(mixed)', 'Output complementary
sensitivity(Hinf)', 'Location', 'NorthEast');

figure(3); impulse(OutputSens_Mxd,OutputSens_Hinf,0:1e-6:0.04);
grid on; hold on
figure(3); Legend('Output sensitivity(mixed)', 'Output
sensitivity(Hinf)', 'Output complementary
sensitivity(mixed)', 'Output complementary
sensitivity(Hinf)', 'Location', 'SouthEast');

figure(4); subplot(2,1,1), plot(PLmxd,'+b'); grid on;
title('Hinf/H2 optimized closed-loop system poles');
figure(4); subplot(2,1,2), plot(PLinf,'*g'); grid on;
title('Hinf optimized closed-loop system poles');

```